GEOMORPHIC AND STRATIGRAPHIC SIGNATURES OF PROTODUNES

A Thesis

by

JOHN DAVID PHILLIPS

Submitted to the Office of Graduate and Professional Studies of
Texas A&M University
in partial fulfillment of the requirements for the degree of

MASTER OF SCIENCE

Chair of Committee,	Ryan C. Ewing
Committee Members,	Chris Houser
	Michael Pope
Head of Department,	Michael Pope

May 2017

Major Subject: Geology

ABSTRACT

Protodunes are precursors to the development of sand dunes and, all else being equal, protodune stratification should occur in the stratigraphic record associated with dune stratification. However, the internal stratification of these little studied bedforms has remained largely unknown and the process which dictate how protodune stratification accumulates and is preserved in the rock record are poorly understood. Here we show that protodune migration generates low-angle stratification that is transitional to angle-of-repose dune stratification, document the occurrence of low-angle stratification in the rock record, and develop a model to explain the distribution of low-angle, protodune stratification in the stratigraphic record. A ground-penetrating radar (GPR) survey conducted across a train of protodunes that give way downwind to angle-of-repose dunes at the upwind margin at White Sands Dune Field, New Mexico shows a spatial transition in dip angles of GPR reflectors from flat-lying to 15° before transitioning to dunes with lee slope angles > 20°. Correlation between individual radar reflections and successive time series topographic datasets establishes that the low-angle reflectors are generated by the migration of the protodunes. Surface grain size fined downwind across the transect from 1.01 mm to less than 0.55 mm. The highest abundance of fine grains coincided with the development of the first angle-of-repose slipface at the most downwind transect. In Paleozoic eolian sequences, < 15° inclined stratification composed of mm-scale wind-ripple laminations and ~10 cm thick, wind-ripple dominated tabular sets, overlain by and interbedded with >15° dune cross-

bedding matches observations of protodunes stratification at White Sands Dune Field's upwind margin. Where present, low-angle stratification consistently occurred at the base of erg growth sequences. The presence or absence of protodunes stratification likely arises due to variable conditions for accumulation at the initiation of the sequence and from variable scour from overriding dunes. From these observations we define a model of the development of low-angle protodune stratification within eolian successions based on process-scale dynamics.

ACKNOWLEDGMENTS

I would like to thank my committee chair and graduate advisor, Dr. Ryan C. Ewing, for his excellent guidance and inspired scientific insight, as well as my committee members, Dr. Chris Houser, and Dr. Michael Pope for their support through the completion of this thesis. Additionally, I would like to thank Roy Bowling for his invaluable assistance and support in the collection, processing and displaying of GPR data used in this study. A round of gratitude is due to Dr. Jeff Nittrouer and his students at Rice University for their assistance in the data collection at White Sands, New Mexico. Many thanks are due to my parents for their support and encouragement throughout the completion of this degree. Finally, thank you to my field assistant Augustine “Augie” Max Olivares for your efforts and support during the field campaign in the Utah dessert.

Thanks also to the Texas A&M Geology and Geophysics department faculty and staff for providing me a world class education. I would also like to extend my gratitude to the American Chemical Society Petroleum Research Fund Doctoral New Investigator Grant # 53544DNI8 for providing the funding which made this research possible. Additionally, many thanks are due to the Greater Houston Scholarship Foundation for providing financial assistance during the course of this degree.

CONTRIBUTORS AND FUNDING SOURCES

Contributors

This work was supervised by a thesis committee consisting of Dr. Ryan C. Ewing [advisor], and Dr. Michael Pope of the Texas A&M Geology and Geophysics department and Dr. Chris Houser of the University of Windsor Earth and Environmental Sciences department.

Grain size data referenced in Chapter II was collected and analyzed by Dr. Jeff Nittrouer of the Rice University Earth Science department. Ground-penetrating radar data was processed primarily by Roy Bowling of the Texas A&M Geology and Geophysics department.

All other work conducted for the thesis was completed by the student under the advisement of Dr. Ryan C. Ewing of the Texas A&M Geology and Geophysics department.

Funding Sources

This work was made possible the American Chemical Society Petroleum Research Fund Doctoral New Investigator Grant # 53544DNI8 to Dr. Ryan C. Ewing.

TABLE OF CONTENTS

LIST OF FIGURES

LIST OF TABLES

CHAPTER I

INTRODUCTION AND PREVIOUS WORKS

Introduction

Protodunes are slipfaceless migrating bedforms and are recognized as the harbingers of fully developed sand dunes (Bagnold, 1941; McKee, 1966; Kocurek et al., 1992; Andreotti et al., 2010). Geomorphically, protodunes emerge from a flat bed of sand and develop into low relief hummocks, which become dunes after migrating several protodune wavelengths (Kocurek et al., 1992). This transition is recognized at the upwind margins of dune fields where a short and dramatic transition in the landscape occurs as protodunes abruptly change into dunes over a few hundred meters and at the inception of dune formation (Lancaster, 1996; Andreotti et al, 2010; Ping et al., 2014). Protodunes fall into a class of slipfaceless bedforms described as sandy hummocks, elementary dunes, dome dunes, and zibars that have been documented as thin-veneers of sand in transit covered entirely by wind ripples (Table 1). These types of slipfaceless bedforms are recognized to make up sandsheets marginal to and between eolian dune sediment transport systems (Warren, 1971; Breed et al., 1979; Fryberger et al., 1979; Kocurek and Neilson, 1986; Momiji et al., 2002).

This research aims to determine the stratigraphic signature of protodune migration in modern and ancient eolian environments in order to relate autogenic processes of bedform development to the stratigraphic record. The objectives of this

Slipfaceless Bedforms:	Author(s):	Year of Publication:	Study Location:	Ancient or Modern:	Significance
Zibar	Holm	1960	Arabian Peninsula	Modern	Defines zibars as dome dunes, low-relief, rolling transverse ridges without a slipface, noting that it is a common form in the central Rub' al-Khali
Zibars	Warren	1971	Tenere Desert, Saharan Africa	Modern	Documents repeating patterns of dunes, 'flats' and zibars which increase in size until the next dune occurs, considerable grain size differences and sorting occur for each feature, with coarsest grains in the 'flats' and finest within the dunes
Sandsheets	Wilson	1973	Saharan Africa, South West Africa, Asia, Australia, Arabian Peninsula	Modern	Divides ergs into four groups: 1) Very Coarse-sand ergs dominated by sandsheets without dunes, 2) Coarse-sand ergs containing dunes without slipfaces, 3) Fine-sand ergs that display dunes with slipfaces, and 4) Mixed-sand ergs where dunes with and without slipfaces are intermixed
N/A	Lupe and Ahlbrandt	1975	Western U.S.	Ancient	Recognizes 'extradune' flat-lying, less poorly sorted stratigraphy in in the subsurface as having a distinct character different from high-angle dune sediments
Sandsheets	Fryberger et al.	1979	Great Sand Dunes National Monument, Colorado	Modern	Characterizes and describes 11 distinct types of low-angle eolian 'sand sheet' deposits primarily made from wind-ripples, Recognizes that 'sandsheets' represent transitional environments and sedimentary processes
Protodune	Lancaster	1982	Skeleton Coast Dune Field, Namibia	Modern	Coarse-grained protodunes are found marginal to the dune field's upwind 'dune wall', as well as between main and subsidiary sand streams feeding the dune field
N/A	Loope	1984	Southwest Utah	Ancient	Recognizes flat-bedded eolian sandstone facies at the base of repetitive dune field growth packages
N/A	Loope	1985	Southwest Utah	Ancient	Flat-bedded sandstones mark the first preserved sediments during dune field genesis, amount of preserved thickness, possibly accumulating in relatively brief period of time compared to total dune field existence
Sandsheets and Zibars	Kocurek and Nielson	1986	Colorado, Mexico, California, Texas, Utah	Both	Vegetation, and coarser grain sizes than typical dune sands are primary factors contributing to prolonged sandsheet accumulation versus dune formation and accumulation, periodic flooding and elevated near surface water tables are of secondary importance
N/A	Chan	1989	Southeast Utah	Ancient	Sheet sand facies found at the base of the White Rim sandstone records the progradational downwind edge that preceded across the area before the main erg mass, as well as other erg margins
Sandsheets	Fryberger et al.	1992	Swakopund, Namibia	Modern	Applies field descriptions and experimental results of granule-ripple deposits to previous descriptions of 'low-angle' sandsheet deposits in order to explain non-sheet like stratal geometries and conspicuous quantities of poorly sorted coarse- and fine-grained strata

Table 1. Summary of previous studies about low-relief eolian bedforms.

Slipfaceless Bedforms:	Author(s):	Year of Publication:	Study Location:	Ancient or Modern:	Significance
Protodunes	Kocurek et al.	1992	Padre Island, Texas	Modern	Dunes develop seasonally through a series of morphologic and dynamic stages from sand patches, wind-ripple protodunes, grainfall protodunes, barchan dunes with grainflow, to mature dunes forming crescentic ridges, bedform growth is accompanied by evolving near surface flow conditions influencing deposition
Protodunes	Lancaster	1996	Namib Sand Sea, Namibia	Modern	Documents the initiation process for sand patches which appear to be protodunes, and tracks their short term development into a more defined morphology
Protodunes	Momiji et al.	2001	Experimental	Modern	Mathematically quantifies the migration speed of a protodune based on its shape
Heaps	Kroy	2002	Experimental	Modern	Mathematically calculates migration rates and critical maximum 'heap' size and minimum dune size based on a variety of fixed conditions
Elementary dunes	Elbelrhiti et al.	2005	Moroccan Sahara	Modern	Surface waves on the surface of barchan dunes reflect morphologic instability related to surface flow conditions. Collisions between barchan dunes produce slipfaceless elementary dunes, at size smaller than the dune's surface wave maximum wavelength, which are ejected downwind.
N/A	Mountney	2006	Experimental	Ancient	Dune field accumulation sequences are marked by sandsheet deposits consisting of low-angle inclined wind-ripple stratification overlying widespread deflation surfaces
N/A	Jordan and Mountney	2010	Southeast Utah	Ancient	Extensive sandsheet facies deposits consist of near flat-lying wind-ripple strata

Table 1. Continued.

research are to determine the internal stratification of active protodunes and document and analyze similar stratification in the eolian rock.

Previous Work - Types of Slipfaceless Bedforms

Slipfaceless bedforms occur in a variety of eolian settings with range of morphologies. Slipfaceless bedforms include protodunes and other bedforms that migrate but do not have an angle-of-repose slipface. Here we provide an overview of

low-relief, slipfaceless morphologies (Table. 1) as context for our definition of protodunes.

Zibars

The Bedouin term ‘zibar’ was codified as a dome shaped, or low relief, rolling transverse ridge without a slipface, forming hard smooth coarse sand surfaces present in many interdune areas as a dominant form in the central Rub’ al Khali (Holm, 1960). Warren (1971), Nielson and Kocurek (1986), and Kocurek and Neilson (1986) expanded on this definition stating that zibars are dominantly coarse-grained, are covered entirely by wind-ripples, have stoss and lee slope angles generally less than 5° and 15° respectively, range from several 10’s of cm to less than 10 m in height, spaced at wavelengths from 150 to 400 m, and occur on sandsheets and dune field margins. Zibar’s broad, low-relief shape most likely arises from the high threshold velocity of the coarse-grained sediment comprising the bedforms surface (Nielson and Kocurek, 1986). At the Algodones Dune Field, California, subtle grain size segregation occurs between zibars containing 0.3 to 0.5 mm sized grains, and adjacent interzibar areas containing grains as large as 1 mm in diameter (Norris and Norris, 1961; Kocurek and Neilson, 1986; Nielson and Kocurek, 1986), both distinctly coarser than the 0.1 to 0.3 mm grain size range typical for eolian dunes with slipfaces (Bagnold, 1941; Wilson, 1973; Ahlbrandt, 1979).

Nielson and Kocurek (1986) also observed coarser sediment concentrating on zibar stoss slopes due to wind deflation, which exposed coarse grains buried by zibar migration during exceptionally strong wind events (Sharp, 1963). Under normal wind

conditions, these coarse sediments are unable to creep up the zibar crest and re-deposit within the lee face and a lag only a few grains thick is left behind as the zibar migrates. This coarse grain lag ultimately becomes interzibar low angle (<5°), sand-ripple/granule-ripple laminae. These low angle laminae commonly display preserved ripple forms due to appropriate admixture of finer grains buried between abundant coarse-grains during gentler wind events, which are in turn buried beneath finer grained lee face deposits of the next successive migrating zibar (Warren, 1971; Nielson and Kocurek, 1986). The arrangement of finer grains nestled between the larger grained foresets imparts a texture appearing as is if the finer grains were "poured-in" to interstitial positions (Fryberger et al., 1992). Coarse layers may also form as preserved ripple foresets (Sharp, 1963; Fryberger et al., 1992). Absence of preserved ripple forms mainly occurs due to insufficient fluctuation in the amount of coarser- and finer-grained sand supplied to the ripple's lee slope (Hunter, 1997). Conversely, medium-sized grains are unable to penetrate and remain trapped between the coarse-grain interparticle cavities effectively are more mobile than finer grains, and move downwind more quickly (Warren, 1971). As a result, while bedforms grow in height, areal coverage and asymmetry downwind, their grain populations winnow a more medium- to fine-size (Warren, 1971; Nielson and Kocurek 1986).

Protodunes

In more recent works many authors utilize the term 'protodune' to encompass the series of morphologic stages eolian bedforms progress before a dune fully develops (Kocurek et al, 1992, Momiji et al., 2002; Kroy, 2002; Andreotti et al., 2010). Protodune

are flat to gently undulating, smooth, sloping, low-relief migrating sand mounds. Protodunes do not have a slipface marked grainflow lamina or have an ephemeral slipface which is frequently covered by wind- or granule-ripples (Lancaster, 1982, 1996; Kocurek, et al., 1992; Cooke et al., 1993; Momiji et al., 2002; Kroy et al., 2002; Andreotti et al., 2010). Protodunes are typically 10's of cm to several m in height, up to 200 m in length, up to 100 m in wavelength. They occur marginally to and within dune fields (Lancaster, 1982; Kocurek et al., 1992, Andreotti et al., 2010). 'Dome-dunes' and sand 'heaps' are considered the same as protodunes in this study based on similar characteristics (Lancaster, 1982; Kroy et al., 2002).

Sandsheets

Sandsheets range from thin irregular veneers of dry sand in transit no more than a few cm above a sand free surface to flat to low-relief, gently undulatory, or irregularly rolling and hummocky sandy aprons/sandy plains covered entirely by wind-ripples where dunes with slipfaces are generally absent or sparse (Wilson, 1973; Fryberger et al., 1979; Kocurek and Nielson, 1986; Chan, 1989; Kocurek et al., 1992). This definition includes Bagnold's (1954) 'sand sheets' and 'gently undulating sand sheets', Wilson's (1973) 'very coarse-sand ergs,' 'coarse-sand ergs,' and 'ripple ergs,' as well as Holm's (1960) 'zibar'.

Sandsheets occur marginal to dune fields in both upwind and downwind locations as transitional facies between high-angle dunes and non-eolian environments, as well as in the same spatial area as dune fields either before their full growth and development of after dune field deflation (Fryberger et al., 1979; Kocurek and Nielson,

1986). Sandsheets closer to an upwind sand source typically are very poorly-sorted with sand grains ranging from greater than 0.65 mm to 0.1 mm, having a significant coarser-grained armored lag component, while more downwind sand sheets are typically finer grained and contain a very fine-grained and mud fraction (Fryberger et al., 1979; Kocurek and Neilson, 1986).

In the ancient rock record sandsheet stratification is thought to represent a marginal aeolian environment. This typically occurs at the upwind margin, as well as a dune field's progradational downwind leading margin (Fryberger, 1979; Lupe and Ahlbrandt, 1975; Loope, 1985; Kocurek and Neilson, 1986; Chan, 1989). Sandsheet stratification contains discontinuous, horizontal to low-angle wind-ripple laminae composed of bimodal granule-to-fine sized grains typically forming beds a few centimeters to 10's of cm thick. Isolated coarse grained, high index ripples less than 1cm thick texturally contrast finer sediments. Adhesion ripples, uncommon breccia layers and wavy mud-draped laminations also occur (Sharp, 1963; Fryberger et al., 1979; Loope, 1845, 1985; Kocurek and Neilson, 1986; Chan, 1989; Condon, 1997). Sandsheet stratification typically unconformably overlies underlying strata and are bounded by gently dipping, curved or irregular erosive scour surfaces several meters in length (Fryberger et al., 1979; Chan, 1989). Sandsheet deposits account for several meters to 10's of meters thick accumulations traceable for 1,000's of meters but also may only extend for 10's of meters in length before pinching out (Kocurek and Neilson, 1986; Chan, 1989; Mountney, 2006). It is important to note the term 'low-angle stratigraphy' is interpreted by Fryberger et al. (1979) as dipping less than 20°, by Kocurek and Nielson

(1986) as dipping less than 15°, and by Chan (1989) as dipping less than 10°. In this study we interpret the term ‘low-angle’ strata as all strata originally deposited dipping less than 15° as a compromise between previous authors.

In summary, flat-lying to low angle wind-ripple dominated strata ubiquitously documented in previous ancient eolianites studies almost always are attributed to sandsheet deposits (Loope, 1984, 1985; Chan and Kocurek, 1988; Chan, 1989; Mountney, 2006; Jordan and Mountney, 2010; Lawton et al., 2015). These studies attribute wide ranges in grain sizes and bed thicknesses to sandsheet deposition without directly relating the morphodynamics of the geomorphic form that created the stratigraphy or any a discussion of the connected depositional processes between low- and high-angle eolian strata. By proposing sand sheet deposition and dune field deposition as separate end-member alternatives for eolian sedimentary transport systems Kocurek and Neilson (1986) addressed the fundamental issue of how enough actively transported sand exists to accumulate thick low-angle sand sheet and zibar deposits, but not initiate dune growth and deposition.. They suggested that dunes were prevented from growing due to conditions adverse to dune growth such as high water-tables, surface cementation or binding, periodic flooding, significant coarse-grained sediment populations and stabilizing vegetation. Of these factors, they argue that vegetation and coarse-grain size are almost certainly the prime factors retarding dune growth.
Some work has recorded the surface and near subsurface sediments on and within hummocky sand sheets, protodunes, dome dunes and zibars (Fig. 1) noting that these features typically are coarse-grained, low relief, asymmetric migrating bedform covered

entirely by wind-ripples and lack a slipface (Warren, 1971, Fryberger et al., 1979; Kocurek and Neilson, 1986; Nielson and Kocurek, 1986; Momiji et al., 2002). Such bedforms were documented to produce preserved stratigraphy that almost exactly matched Fryberger et al.'s (1979) and Kocurek and Neilson's (1986) stratigraphic descriptions of sandsheet strata. Our hypothesis differs somewhat from these previous works in that we suggest protodunes are a necessary step along the pathway to dune development, rather than an alternative end member of the eolian system, producing increasing steeply dipping, low- to moderate-angle stratigraphy until full dune growth is achieved.

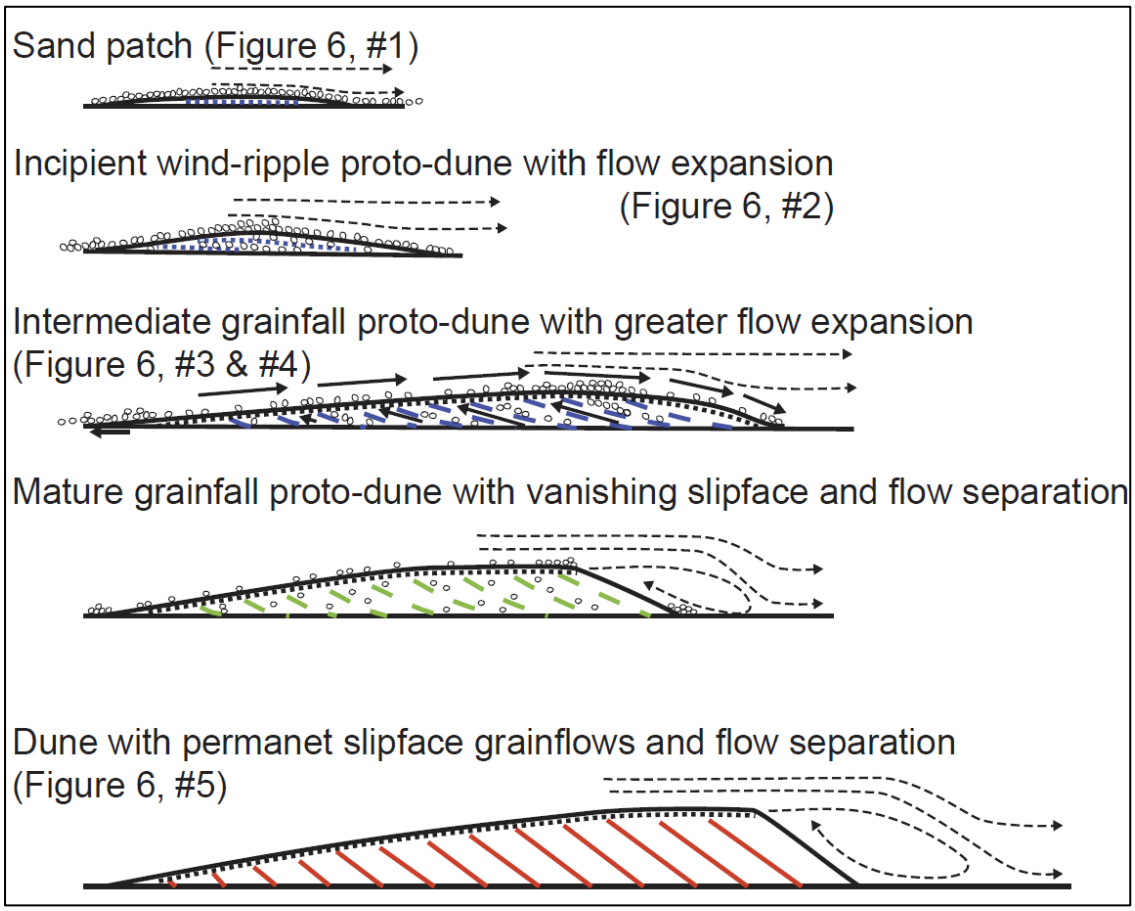

Figure 1. Schematic showing current models for the geomorphic, aerodynamic, and stratigraphic evolution for protodune growth stages. Blue lines correspond to low-angled (<5°) stratigraphy, green to moderate-angled stratigraphy (5<15°), and red to high-angled (>15°) stratigraphy. Stippled lines indicated wind-ripple stratification, dashed lines for grainfall stratification, and solid lines for grainflow cross-stratification. Winnowing grain size show by decreasing amount of representative coarse grains within successive bedforms. Schematic of grain recycling through a migrating protodune is shown within the intermediate grainfall protodune where arrows represent grains creeping along the wind-rippled protodune surface, incorporation by lee face burial, and later exhumation along the stoss slope. Modified from Sharp, 1963 and Kocurek et al., 1992.

CHAPTER II

PROTODUNE STRATIFICATION AT WHITE SANDS DUNE FIELD, NEW MEXICO

Protodunes are low-relief slipfaceless bedforms that develop before dunes develop (Kocurek et al, 1992, Momiji et al., 2002; Kroy, 2002; Andreotti et al., 2010). The evolution of protodunes has been documented where dune fields grow over observational time scales (Kocurek et al., 1992; Ping et al., 2014). However, the upwind margin of dune fields shows the spatial transition from protodunes to dune. We analyze the upwind margin of White Sands Dune Field to characterize the spatial and temporal evolution of protodune migration.

White Sands Dune Field, Tularosa Basin, New Mexico, USA

The White Sands Dune Field (Fig. 2) is the largest known gypsum dune field, covering between 400-500 km^2 within the Tularosa Basin, southern New Mexico (McKee, 1966; McKee and Douglass, 1971; Fryberger et al., 1988; Langford, 2003; Kocurek et al., 2007). The north-south trending Tularosa Basin formed within the elongate, extensional Tertiary Rio Grande Rift (Fryberger, 2000; Langford, 2003). Locally, the San Andres and Sacramento Mountains flank the topographically enclosed basin, restricting groundwater outflow (Langford, 2003). During the latest Pleistocene Lake Otero occupied the western part of the basin (Langford, 2003). This lake began to dry up approximately 7,000 years ago with the onset of regional aridity, today the basin is filled with approximately 20 playa lakes.

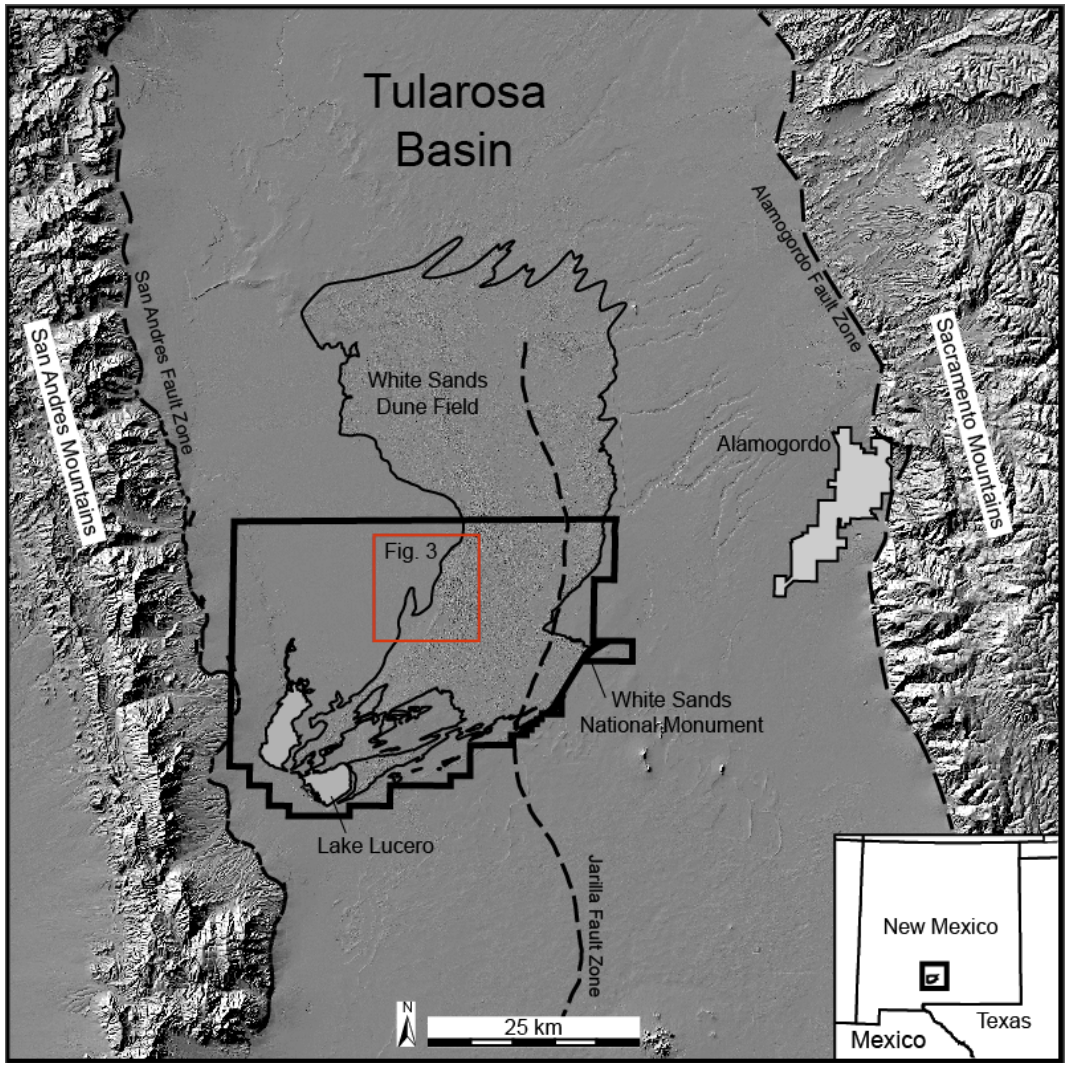

Figure 2. Location of the White Sands Dune Field within the Tularosa Basin, New Mexico. The fault bound Tularosa Basin lies within the much larger Rio Grande Rift. Note the locations of the White Sands National Monument, and the modern playa Lake Lucero, as well as location of figure 3 along the dune field's western upwind margin.

The largest of the modern playa lakes is Lake Lucero, which occupies the topographically lowest portion of the basin and lies upwind of the modern dune field (Langford, 2003; Kocurek et al., 2007).

The drying of Lake Otero most likely occurred in a stepwise manner as seen in

the successive 1,215 m, 1,211 m, 1,206 m, 1,200 m, L1 (~1,200 m elevation), L2 (1,191 m elevation) and modern shorelines (1,185 m elevation) each marking an increase in regional aridity (Langford, 2003; Kocurek et al, 2007; Baitis et al., 2014). The modern dune field most likely initiated during punctuated deflation from the L1 to L2 shorelines dating slightly before 6,000 years ago, cutting through Pleistocene bedded evaporates (Allmendinger, 1972; Langford, 2003). At that time a short constructional episode leading to rapid dune field expansion corresponded to a greatly increased sediment supply and favorable wind regime (Kocurek, 1998; Lancaster et al., 2002; Langford, 2003). The modern dune field's lagged sand flux from remaining Lake Otero sediments and contemporary playa sediments supplies the dune field with enough sand to keep the dune field in a condition of stasis, neither expanding or contracting (Langford, 2003; Kocurek et al., 2007).

Gypsum supplied to the dune field from a range of sources. Gypsum leached from the evaporite-rich Permian strata exposed within the surrounding San Andres and Sacramento Mountains and in the subsurface is carried via groundwater to the basin center and is precipitated at the surface as gypsum (Allmendinger, 1972). Interactions between Paleozoic carbonate sequences and sulfate rich volcanic rocks in the subsurface may also contribute to the production of gypsum within the basin (Szynkiewicz et al., 2010). This leaching and groundwater transport process continues through the present, however at a much slower rate as reduced evaporation and precipitation wick groundwater brines to the surface of playa lakes upwind of the active dune field (Allmendinger, 1971, 1972; Langford, 2003; Kocurek et al., 2007).

The active dune field abruptly emerges from the upwind alkali flat deflation plain, above the L1 shoreline. The heart of the dune field contains crescentic and transverse barchanoid dunes while parabolic dunes form to the north, east and south, and protodunes and sand sheets lie to the west (Langford, 2003; Kocurek et al., 2007; Jerolmack et al., 2012). The crescentic dunes follow a 075° transport direction (Ewing et al., 2006), which is borderline transverse to the Fryberger's (2000) and Hunter et al.'s (1983) measured wind resultant of 60° at the nearby Holloman AFB. Dominant southwesterly winds during the winter-spring, coupled with subordinate north-northwesterly winds during the fall-winter and south-southeasterly winds during the spring-summer rework active dune topography and result in an average 3.6 m/yr resultant migration rate (McKee and Douglass, 1971; Langford, 2003; Kocurek et al., 2007; Pederson et al., 2015). Active dunes become sparser downwind indicating a rapid decline in sand flux 1-2 km from the upwind margin and then decrease more slowly for distance up to 10 km (Jerolmack et al., 2012). Downwind increasing grain-maturity and decreasing grain size trends are hypothesized to result from grain abrasion and decreasing sand transport capacity and efficiency, only transporting the smallest grains furthest (McKee, 1966; Langford, 2003; Jerolmack et al., 2012).

Low relief, wind-ripple covered protodunes occur on the dune field's unvegetated upwind-margin, (Langford, 2003; Kocurek et al., 2007). These incipient bedforms represent a transitional facies from playa to dune environments (Fryberger, 2000). This area is characterized by coarse grains and coarse-grained granule ripples along with abundant wind ripples (Fryberger, 2000).

Methods

Ground-penetrating radar (GPR), RTK (real-time kinematic) GPS, grain size and can provide insight into the internal structure and evolutionary history of sand dunes (Harari, 1996; Bristow et al., 2000; Botha et al., 2003). Because the internal bedding in various types of eolian morphologies can differ significantly, clear imaging of the internal structure can help identify various stratigraphic features unique to specific bedforms (Mainguet, 1984; Botha et al., 2003). A transmitting antenna placed on the ground surfaces propagates short pulses of electromagnetic energy (radio waves) into the ground, while a receiving antenna records returning waves generated from impedance contrasts across subsurface interface such as juxtaposed strata (Harari, 1996). Lower frequency signals are more effective for imaging deeper structures, whereas higher frequency signals are more suited for imaging shallower, very fine sedimentary structures (Harari, 1996, Botha et al., 2003). The velocity of signal propagation is governed by the imaged material's dielectric constant (Parkhomenko, 1967). If the velocity of the propagated wave is known, it is possible to determine depth to a particular reflector which is proportional to the two-way travel time of the subsurface feature. In this manner, the results of a collected radar section are equivalent to a zero-offset common mid-point stack in seismic reflection exploration (Harari, 1996).

A 784 m long GPR and GPS transect oriented 075° azimuth was collected at the active upwind margin at White Sands National Monument, New Mexico (Fig. 3 & 4). The transect aligned with the primary southwesterly winds and was orthogonal to the dominant dune orientation (Ewing et al., 2006). In this orientation, the dip of cross-strata

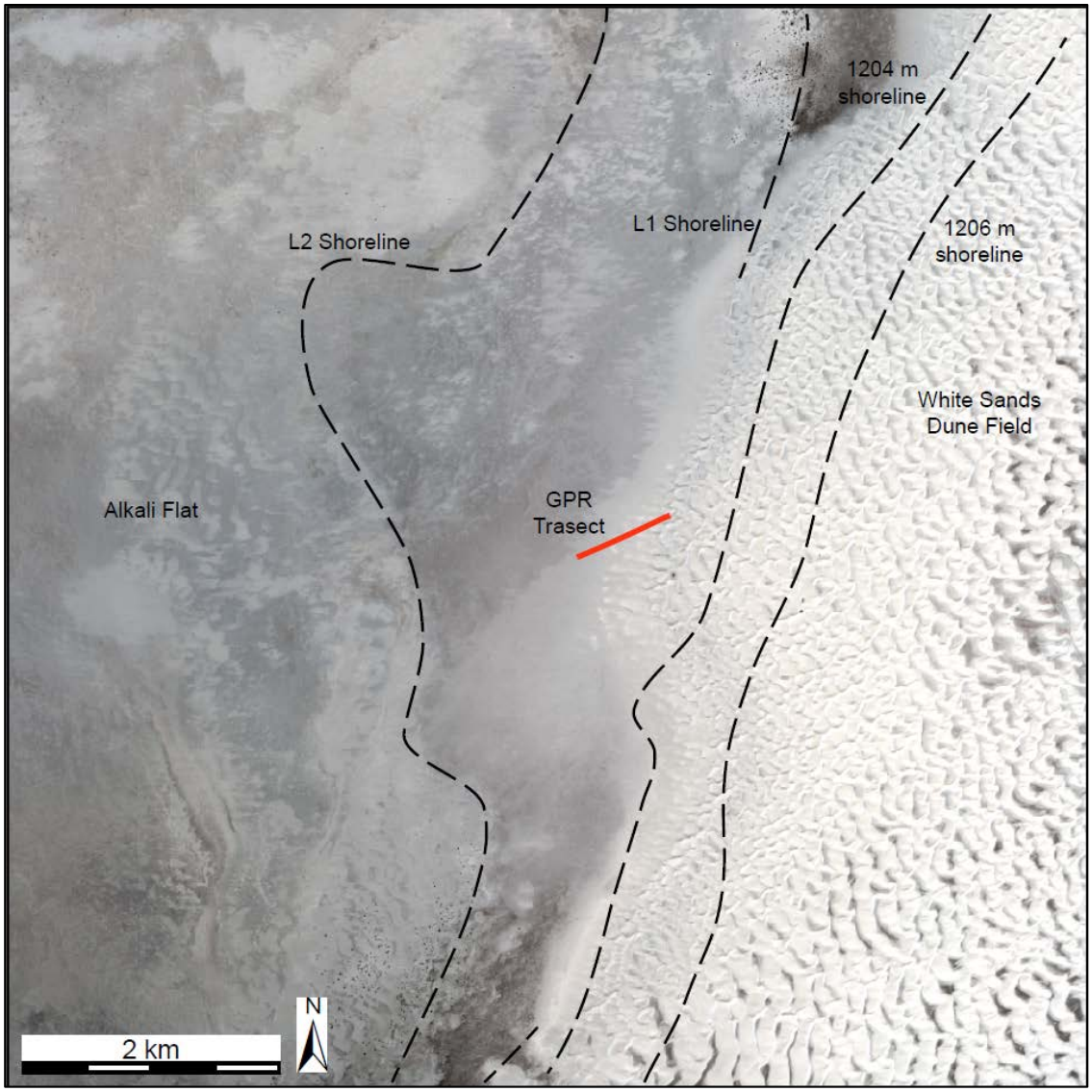

Figure 3. Satellite image showing the location of the surveyed transect along the White Sands Dune Field's western, upwind margin. Note the correspondence between the Lake Otero L1 and L2, 1204 m, and 1206 m paleoshorelines from Langford (2003) and Baitis et al. (2014), and the Dune Field's upwind margin. The Alkali Flats area extends westerly to modern playa lakes, and the dune field develops into a core of barchan dunes to the east.

and bounding surfaces are best visualized. However, any crestline curvature that could generate trough cross-strata or an oblique transect through a crest oriented

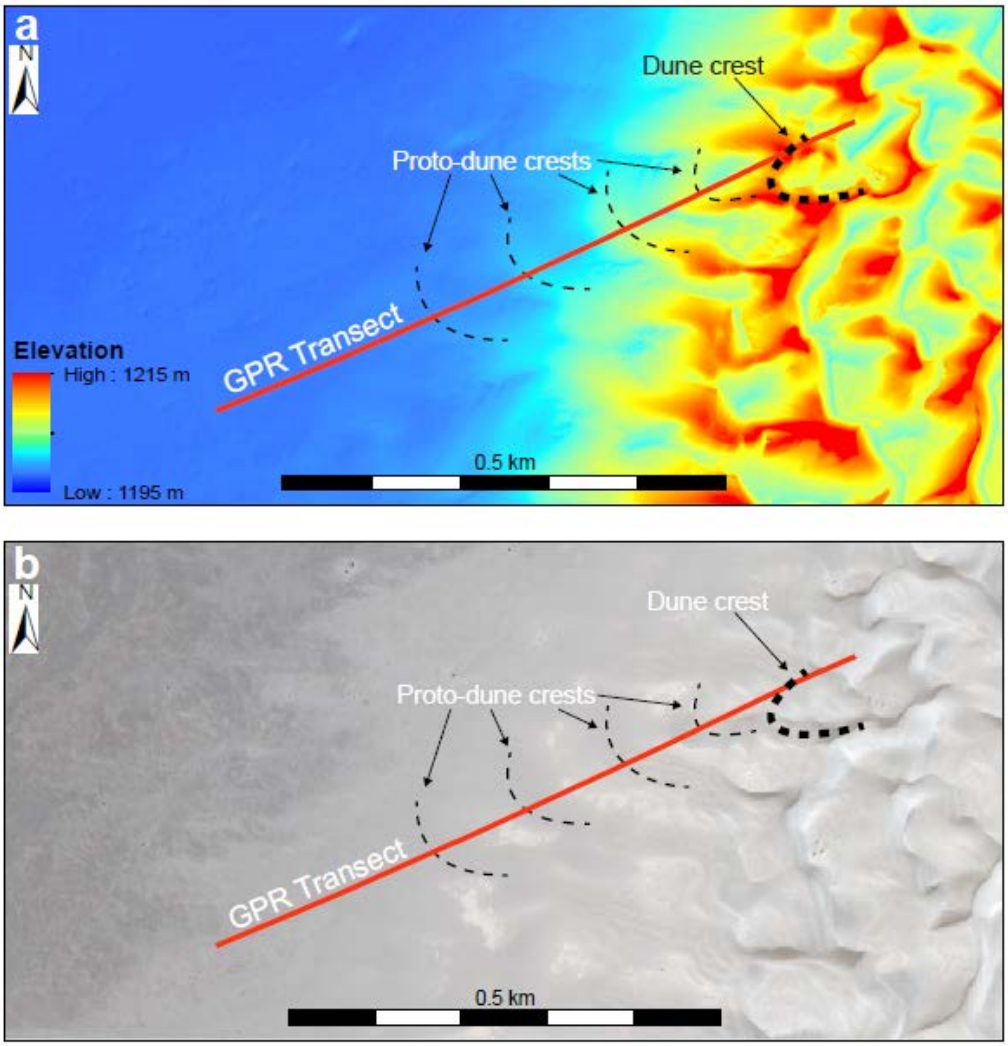

Figure 4. Protodune and dune morphology along White Sands Dune Field's upwind margin. Note Protodune and dune morphology and crestline orientation in each of the following figures. (a) Digital elevation model of study area showing warmer colors as higher elevations. (b) High resolution aerial imagery of study area. Amount of sand cover increases to the right of the image. (c) Field photo looking southwest, and upwind along the approximate area of the surveyed transect. Note extremely subdued relief upwind of the first dune in the lower left of the image.

non-transverse to the 075° transect would generate apparent dip angles (Bristow, 2009). The data were collected with a sled mounted, 200 MHz Sensors and Software pulseEKKO Pro GPR operating in a bi-static collection mode, wherein a signal is

Figure 4 Continued.

transmitted by one antenna and received by another antenna separated by approximately 1 m along the sled (Fig. 5a). In order to accomplish an acceptable balance of depth of penetration and detail of reflection signals, radar trace samples were collected at 0.1 m intervals along a measuring tape, based on the Nyquist sampling interval, which is one-quarter of the wavelength in the ground, to ensure no spatial aliasing from under-sampled subsurface features (Bristow, 2009).

Topographic measurements required for static elevation corrections to the GPR data were collected from the upwind alkali-flat sediments, downwind past the first true distinguishable slipface, and on to the first true dune's stoss slope. An approximate 0.1 m spacing along a tape measure was used for topographic measurements to best coincide with the sample spacing used in GPR surveying, as well as for capturing very fine resolution measurements at slope breaks and areas with high topographic variation. The

topographic survey utilized differential GNSS measurements incorporating Real Time Kinematic Corrections broadcast from a local, stationary base-station to a mobile "rover" unit used for data collection. This ensured observed horizontal error vectors below 0.003 m and observed vertical error vectors below 0.01 m.

Data clean-up was required for collected topographic data in order to apply correct topographic corrections and write valid trace header files for the GPR data. This was done using a 3-point window smoothing filter, iterated four times. Following the fourth iteration no significant smoothing was detected between topographic measurements, and the points were determined to accurately reflect the survey profile. Additionally, a spline interpolation method located all points exactly 0.1 m apart from one another along the survey profile. The exact 0.1 m distance spacing along the topographic profile provided realistic elevations used in topographic correction, as well as horizontal locations for writing header files, at each trace location.

To extract an image appropriate for interpretation, de-wow, background subtraction, band-pass filtering schemes were applied along the length of each trace, removing low frequency inductive effects, unwanted horizontal reflections due to the air wave direct arrival and signal ringing within the receiving antenna, as well as frequency artifacts 50% above or below the 200 MHz center frequency (Fig. 5b). Two-way travel times were converted to depth measurements using a dielectric constant between 5 and 10 (Young and Frederikse, 1973) to empirically derive a 0.122 m/ns migration velocity. This resulted in a vertical resolution around 0.15 m which agrees with the theoretical resolution for a 200 MHz survey in damp sand as described by Jol and Bristow (2003).

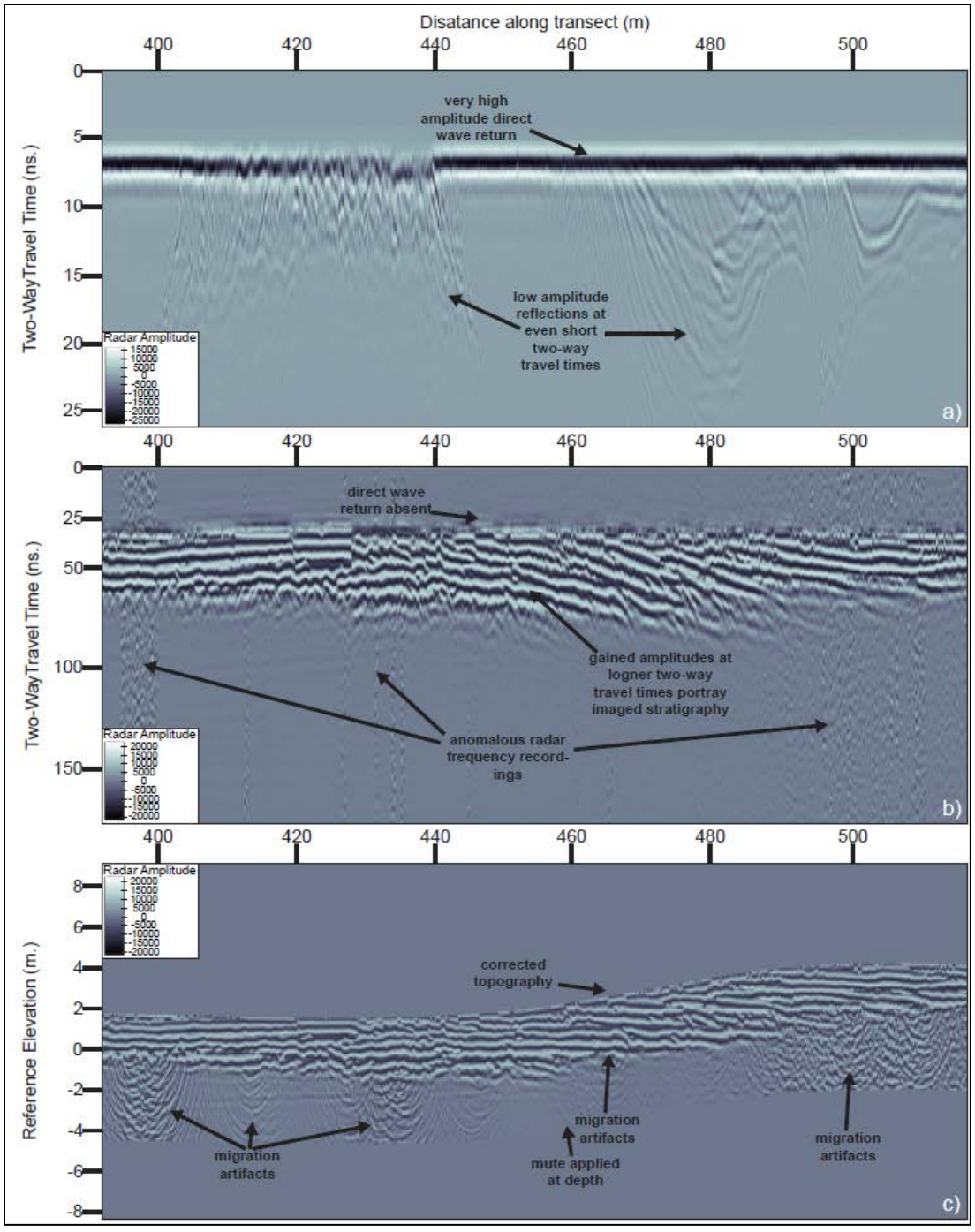

Figure 5. Radargram (using 200-MHz antenna) showing a cross-sectional view of the White Sands Dune Field's Upwind Margin. (a) Raw data. (b) Gained data without elevation correction. (c) Migrated data with elevation correction.

Additionally a static topographic correction (Fig. 5c) shifted each trace to their correct elevation along the survey line as well as aligning reflections to their true location with respect to one another, reflecting the realistic stratigraphy. Automatic Gain Control applied to the data applies a constant amplitude envelope for each trace but highlights each reflector within the data, desirable for stratigraphic delineation and interpretation. Finally, the GPR traces files were converted to .segy format for interpretation within Petrel software.

First order bounding surfaces were identified within the data based on definitions by Brookfield (1977), as well as radar facies and unique patterns of terminating reflectors (Fig. 6). From the interpreted stratigraphic packages, dip angle trends were easily observable and measured to assess the stratigraphic development along the surveyed transect. Additionally, this data was overlain by yearly time series LiDAR topographic surveys, ranging from January, 2009 to 2016, to track the geomorphic evolution through time to the point of GPR survey during 2015. Although the various LiDAR topographic data sets were collected in a variety of vertical and geodetic datums, all elevations were collapsed to the same point at the start of the transect to generate common reference elevations along identical transects. Because various topographic measurements are referenced to the exact same spatial location, adjusting topographic measurements to a common reference elevation significantly aligns the various data enabling suitable analysis.

Anomalous radar facies

Throughout the data, irregular radar reflections closely resemble downward

expanding, stacked semi-circles (Fig. 7, Figure 8c & d). These anomalous reflections most likely are erroneous data artifacts recorded from the radio wave frequencies used in simultaneous RTK GNSS topographic surveying and modified in the migration and gaining processes. Before migration occurs in figure 5b, these data artifacts are essentially anomalous radar return values recorded by the receiving antenna, displayed in time as points and later 'smeared' into semi-circles during migration. While these values are almost insignificant in their initial radar amplitude returns (Fig. 5a), the gaining processes applies approximately equivalent amplitude values to all the recorded measurements, resulting in an anomalously high amplitude appearance.

GPR Survey Results

Radar reflection facies

Horizontal to sub-parallel, flat-lying radar facies

Radar reflections dipping close to 0° dominate the surveyed transects at the edge of Alkali Flat as well as the first encountered upwind surface bedforms (Fig. 7). These radar reflections extend laterally nearly 100 m before terminating at low angles (<5°) into other flat-lying reflections. Reflections terminate along relatively continuous low-angle (<15°) reflections and form distinct, continuous reflection termination patterns when no traceable continuous first order bounding surfaces exists. These radar reflections marginal position, low-angle geometries and lateral continuity closely resembles the low-angle stratigraphic geometries identified by 'wind-ripple' like stratigraphy of larger granule-ripples, Kocurek's (1992) incipient sand patches, and sandsheets (Sharp, 1964; Wilson, 1973; Fryberger et al., 1979; Loope, 1984, 1985;

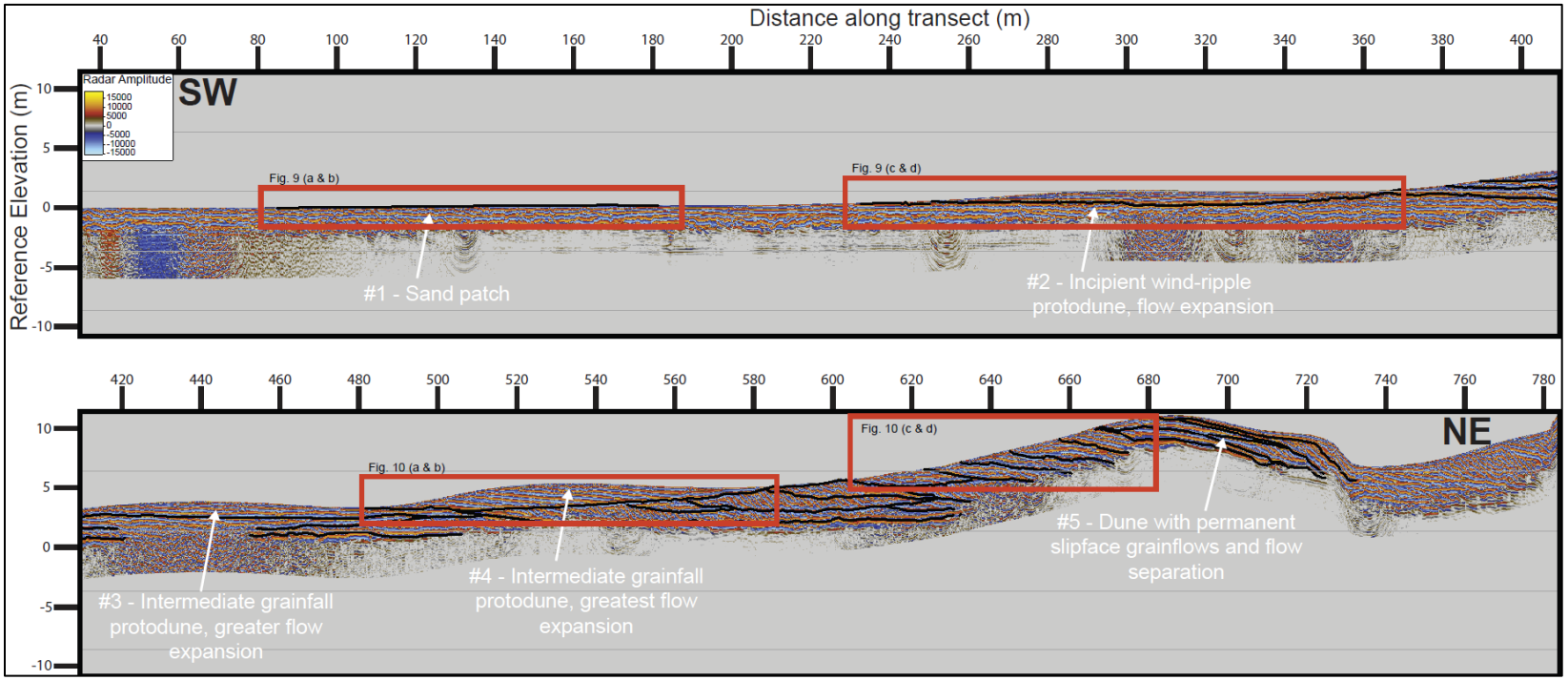

Figure 6. Overview of ground-penetrating radar reflection data collected along the transect in fig. 4. Processed radar reflection data is colored with positive amplitude radar reflections as warmer colors and negative amplitude reflections as cooler colors. Elevations along the left side of the image read from a reference elevation of 0 m corresponding to the essentially flat topography of the Alkali Flats area upwind. Preliminary interpretations of first order bounding surfaces are show by black lines and bound packages of various radar reflection geometries

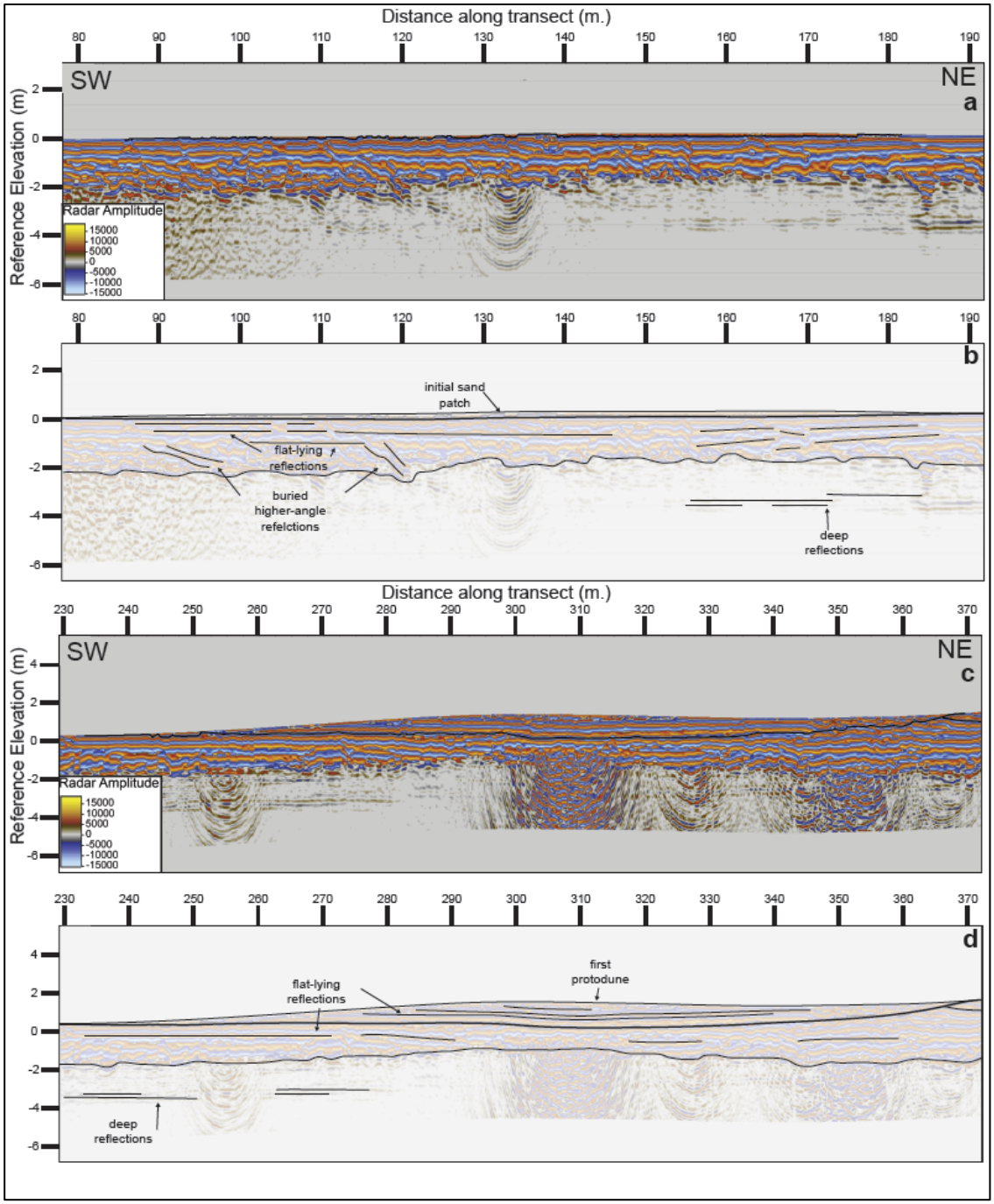

Figure 7. Cross-sectional view of a wind-rippled sand patch and the first downwind protodune seen in figure 6. (a) Radargram of upwind sand patch. (b) Radar facies interpretations of upwind sand patch. (c) Radargram of first upwind protodune. (d) Interpretations of radar facies within first upwind protodune.

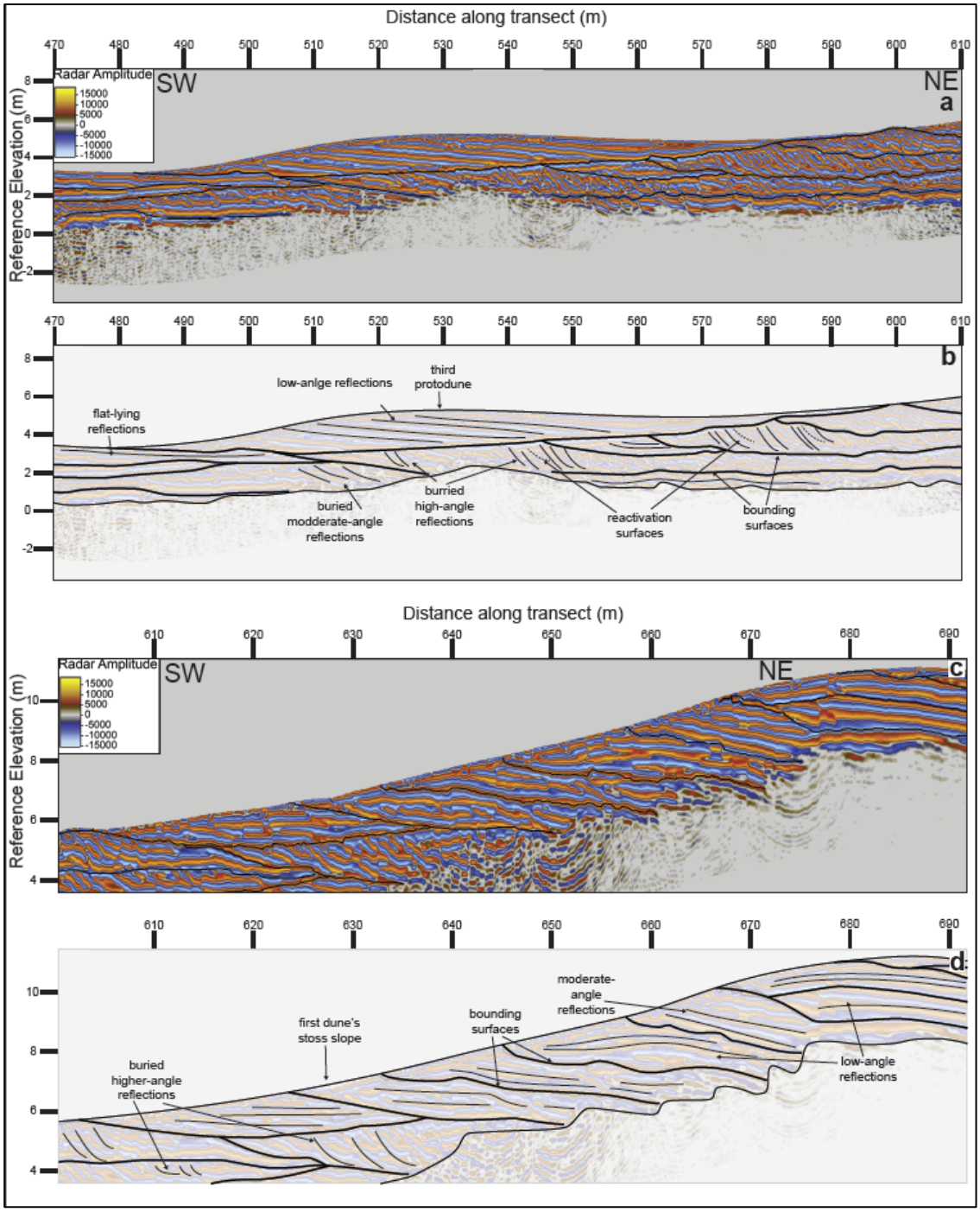

Figure 8. Cross-sectional view of third downwind protodune and first encountered dune's stoss slope seen in figure 6. (a) Radargram of third downwind protodune. (b) Radar facies interpretations within protodune. (c) Radargram of first encounter dune's stoss slope (d) Interpretations of radar facies within first encountered dune's stoss slope.

Kocurek and Nielson, 1986; Chan, 1989; Mountney, 2006). However, the surface morphology of the bedform captured in figure 7c, and 7d, comprised entirely of flat-lying radar facies reflections resembles an incipient protodune, low zibar, or sand 'heap' (Holm, 1960; Warren, 1971; Lancaster, 1982; Kocurek and Nielson1986; Nielson and Kocurek, 1986; Kocurek et al., 1992; Cooke et al., 1993; Lancaster, 1996; Momiji et al., 2002; Kroy et al., 2002; Andreotti et al., 2010).

Low- to moderate-angle radar facies

Subsurface radar reflections dipping greater than 0° less than 15° occupy the most windward positions within first-order bounded subsurface reflector packages (Fig. 7 & 8), generated by the migration of dunes and protodunes (Brookfield, 1977). Also, the most downwind protodune and first dunes' stoss surface and crest contain completely low- to moderate-angle radar reflections ranging from close to 5° to less than 15° (Fig. 8). Low- to moderate-angle geometries typically imply sandsheet stratification, however the most upwind and sandsheet-like surfaces have flat-lying reflectors rather than low-angle reflectors. Low- to moderate-angle reflectors only occur within intermediate and more developed, higher-relief mature downwind protodunes with lee slopes at angles at angles less than 5°, well within the 0° and 22° range reported for protodune, zibar and 'heap' lee slopes (Kocurek et al., 1992; Kroy et al., 2002; Andreotti et al., 2010).

High-angle radar facies

Radar reflections dipping greater than 15° dominate the surveyed transects subsurface positions beneath protodunes upwind of the first encountered dune, as well as

the first encountered dunes surface and subsurface lee slope (Fig. 8). These radar reflections display a concave upward to planar geometry typically decrease in dip towards their base and onlap basal first order bounding surfaces. The high-angle, concave upward to planar geometry is interpreted as dune lee face stratification (Harari, 1996; Bristow et al., 2000; Botha et al., 2003). Identifying this radar facies within the first developed dune's lee slope supports this interpretation. Additionally, the first developed dune's lee face exhibits progradational geometry of high-angle radar reflections building downwind. Higher-angle reflections and radar reflection termination patterns divide specific packages of low-to-high angle radar reflections (Fig. 8a & b). Angular relationships between these surfaces and the radar reflection packages they sub-divide closely resemble Brookfield's (1977) reactivation surfaces, which cut across small bundles or intrasets of cross-laminations often at lower angles than the laminae themselves.

Radar reflection dip angle patterns

After measuring all radar refection dip angles along the surveyed transect, distinct radar facies showed ordered variation in dip angle downwind (Fig. 9). As seen in Fig. 9c radar reflection dip angles within surface bedforms increased in dip angle from 0° to 5°along the transects first 700 m before dramatically increasing to greater than 15° within the remaining 84 m, which is coincident with the first fully developed dune's slipface. Subsurface radar reflection dip angles show a similar dramatic increase at a more upwind position, with the most windward high-angle radar reflection positioned

approximately 400 m upwind of the surveyed active dune's slipface, and may correspond to an old position of the upwind margin.

Topographic overlay comparison

Correlation between the time series LiDAR data transects, which range over 9 years, and the GPR data revealed relationships between the topography and preserved stratigraphy (Fig. 10). From the most upwind discernable sand patch, to the bedform encountered just before the first surveyed dune, protodunes measure 0.18 m, 1.12 m, 1.28 m, and 1.96 m in height, and 99.42 m, 136.54 m, 120.73 m, and 119.01 m, in downwind length respective to downwind position. For each protodune surveyed, the past lee slopes aligned almost exactly with preserved stratigraphy within the bedform. Although lee slopes angles and bedform asymmetry gradually increase downwind, three upwind protodunes (Fig. 6 #2, #3, & #4) surveyed did not show significant differences in crest-to-crest migration rates. The bedform migration rates from upwind to downwind were 15.912 m/yr, 18.912 m/yr, and 16.476 m/yr. This is considerably greater than the dune field's average 3.6 m/yr migration rate (Pederson et al., 2015).

Complex changes in reflector dip angles within the first surveyed dune's crest appear to correspond to the initiation of a secondary protodune spawned atop a well-developed protodune's crest. Interestingly, in the area between the first encountered, upwind protodune and the Alkali Flats area, irregular micro-topography, composed of sand patches no larger than 10 cm in height, did not show much correlation between successive topographic datasets. Field observations concluded that transitory, irregular sand patches commonly less than a few cm high dominated this area, changing location

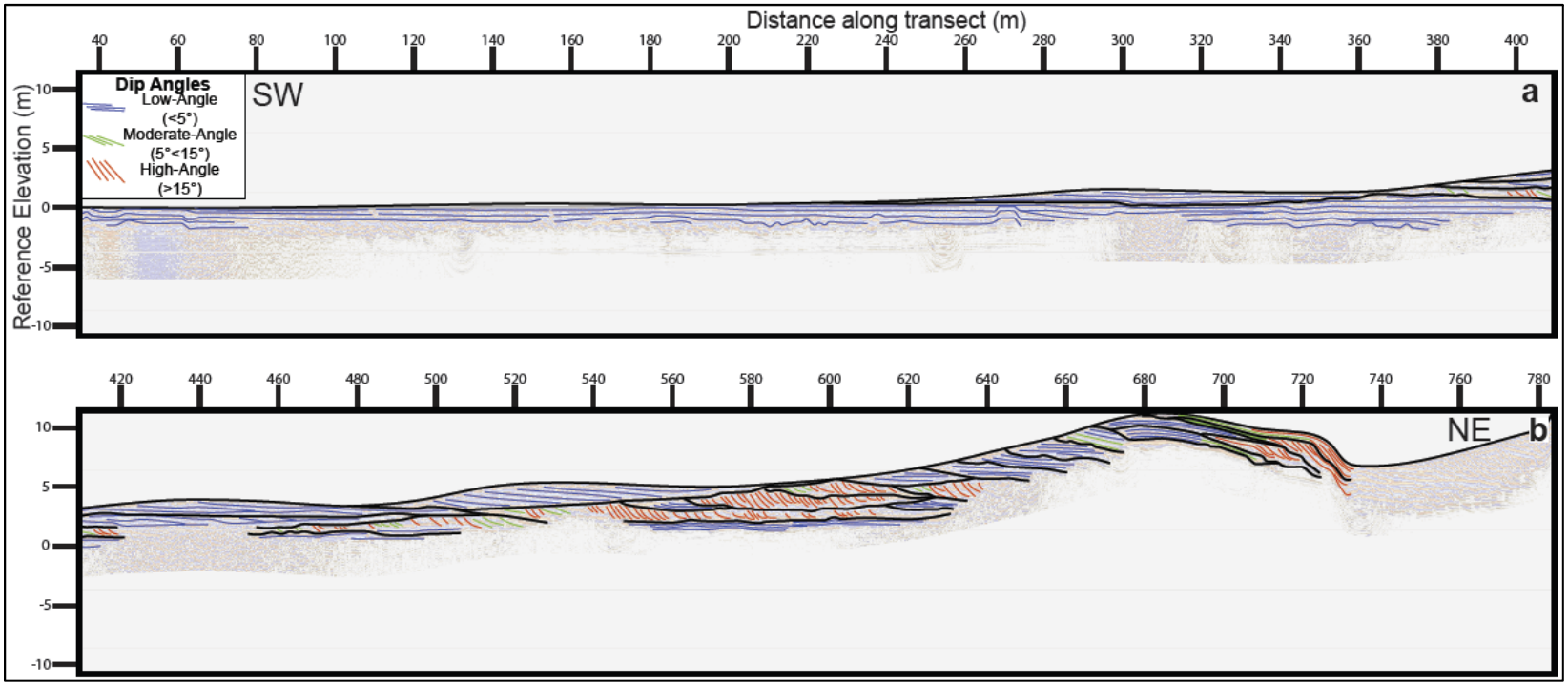

Figure 9. Stratigraphic dip angle evolution along the surveyed transect. (a) Most upwind portions of the surveyed transect displaying predominately low angle stratigraphy. (b) Most downwind surveyed portions of the surveyed transect displaying much more varied dip angles. (c) Graphical representation of dip angles data along the surveyed transect. Solid circles represent angles measured within the active surface bedforms opposed to preserved subsurface stratigraphy (open circles).

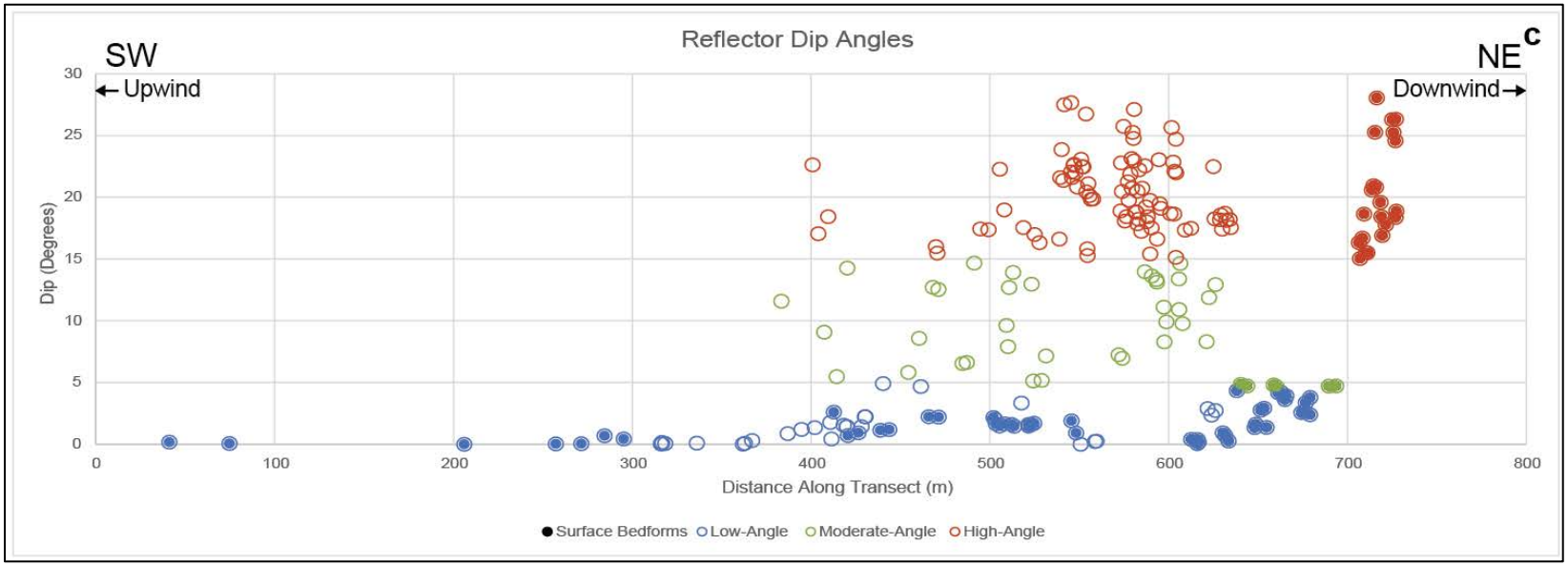

Figure 9 Continued.

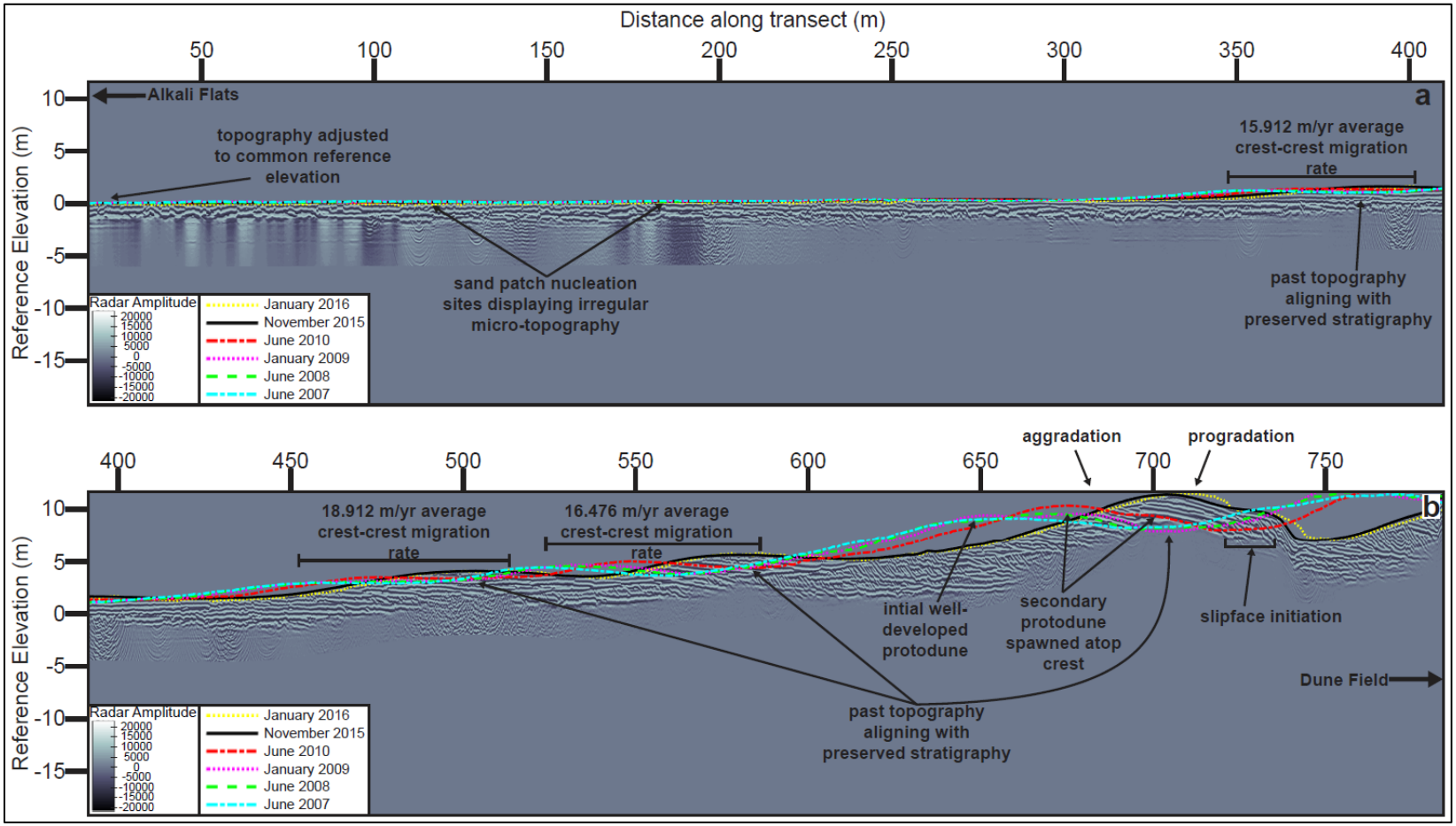

Figure 10. Radar reflection data overlain by time series topography data. (a) Most upwind portions of the surveyed transect. Note relatively flat, irregular micro-topography in areas of sand patch initiation. (b) Most downwind portions of the surveyed transect. Note progressive protodune crestline migration and profile evolution corresponding to increasing stratigraphic dip between successive years, as well as slipface initiation between 2010 and 2015 data sets.

and shape significantly between the survey's different days, possibly explaining the poor correlation between these less permanent features in data sets separated by several months to years.

Grain size observations

Further field observations and grain size collections along the surveyed transects surface showed strong spatial grain size variations. Grain sizes steadily decreased downwind from an average coarse-grained sand (d50 ~ 9 mm) at the most upwind sand patches, to a distinctly more upper medium- to medium-sized sand (d50 ~ 5 mm) population at the first encountered active dune's crest. The surface of the most upwind sand patch nucleation site, and stoss slopes of the surveyed protodunes displayed coarse-grain enrichment compared to grain size populations on the protodune lee slopes. Alternatively, exceptionally high medium to fine-grained (d50 ~ 3 mm) fraction frequently collected leeward of small shrubs and other small topographic features such as patches of vegetation acting as sand traps.

Discussion

Protodune morphology and stratigraphy

The bedforms surveyed upwind of the first encountered dune have typical protodune morphology, and very closely correspond to the dimensions Lancaster (1982) documents upwind of the Namib sand sea for similar low-relief morphologic features, Kocurek et al.'s (1992) dimensions for seasonal protodunes measured at Padre Island, Texas, Andreotti et al.'s (2010) critical protodunes measured in Saudi Arabia and the Atlantic Sahara, as well as Kroy et al.'s (2002) experimentally derived critical size for

steady state ‘heaps’. Kroy et al. (2002) also notes that protodunes’ plan-view aspect ratio (Length : Width) increases with increasing bedform height. While the measured GPR transect only portrays 2-D downwind length, quick inspection of a digital elevation model at the upwind margin (Fig. 4a) confirms that the protodunes surveyed in this study also decrease in width downwind, increasing their plan-view aspect ratio, while increasing in height. Additionally, the surveyed protodunes lee slopes increase from almost 0° to just under 5°, mirroring Kocurek et al.’s (1992) protodune lee slope evolution leading to increased asymmetrical morphology.

Internal reflector geometries within the surveyed protodunes, which we interpret to represent evolving protodune stratigraphy, progressively increase in dip angle from flat-lying, to moderate-angles downwind. Because the most upwind sand-patch (Fig. 6 #1), and upwind two protodunes (Fig. 6 #2 & #3) are comprised entirely of flat-lying radar reflections, it is reasonable to interpret some degree of the horizontal, flat-lying radar reflections as protodune stratification as well. Additionally, the third most downwind protodune’s stratification (Fig. 6 #4) displays increased dip angles bordering moderate angles, and therefore we interpret protodune stratigraphy to encompass at least some moderate-angle subsurface stratigraphy. Also important to note, high-angle progradational stratigraphic geometries within the first developed dune’s lee slope (Fig. 6 #5) mirror similar high-angle subsurface radar reflections positioned 400 m upwind, suggests that buried moderate- and high-angle stratification may document previous dune field margin positions, or at least that in the past dunes deposited stratigraphy in a

more upwind position than they do currently, indicating this margin is an erosional-type margin.

Grain size fractionation

Grain sizes distributions measured in this study echo Warren's (1971), Lancaster's (1982), and Nielson and Kocurek's (1986) similar local and regional grain size distributions, pointing to a natural processes responsible for preferentially sorting sand grains based on local topographic influences. We propose that process-scale interactions between a protodune's wind-rippled surface and the near surface flow effectively sort sand grains. As wind flows up a protodune's stoss slope there is slight flow convergence and acceleration, increasing shear velocity (u^*) causing erosion and transport, with some deposition occurring at the dunes crest promoting protodune slope break growth and asymmetry. After wind passes the protodunes crest, flow expansion and deceleration occurs across the steepening, increasingly asymmetric slope break, decreasing shear velocity and driving sand deposition (Nielson and Kocurek, 1986; Kocurek et al.1992; Andreotti and Claudin, 2007). Where shear velocity (u^*) along protodune stoss slopes is not great enough to transport coarser grains past the protodune crest, only the finest grains are transported onto the lee slope, which causes lee slope fine-grained enrichment (Nielson and Kocurek, 1986). Medium- and fine-sized grains are easily winnowed and transported downwind from the protodune crest (Warren, 1971; Neilson and Kocurek, 1986).

Lee slope developments

The distribution of eolian transport and depositional processes over a bedforms'

surface dictate the internal structure of deposited sediment (Hunter, 1977; Nielson and Kocurek, 1986; Kocurek et al., 1992; Andreotti et al., 2010). Evolving process-scale interactions between the depositional surface and the transporting fluid result in increasing leeward flow expansion and separation, increasing lee slope angles, and drive protodune growth (Nielson and Kocurek, 1986; Kocurek et al., 1992; Andreotti and Claudin, 2007). We propose downwind increasing stratigraphic dip angles (Fig. 9) record this this relationship.

As seen in figures 7 and 8, topographic profiles for mature protodunes develop considerable asymmetry coincident with increasing radar reflection dip angles within the surface bedforms. Prior to this well-developed protodune growth stage, only low-angle stratification dominates protodune depositional processes, influenced by interactions between cm high wind-ripples covering the protodunes, the grains within the ripples and the transporting wind (Sharp, 1963; Nielson and Kocurek, 1986). Thus, while protodunes grow from nucleation sand patches to mature protodunes they produce flat-lying to low-angled stratification from bedforms ranging in several cm in height, 10's of cm in height to several m in height, providing and alternative explanation to theories that such stratification only arises from nearly flat lying sand patches/sand-ripples, granule-ripples or sandsheets. The significance of these observations is that late growth-stage flow expansion/incipient flow separation produces stratigraphy unique to protodunes, capable of accumulating wherever dunes grow. Additionally, moderate-angled protodune stratification may occur intercalated with more common high-angle grainflow stratification (Fig, 7) depending on level, and consistency of flow separation/flow

expansion occurring past the protodune's crest.

Relation to sandsheet stratigraphy

Stratigraphic geometries measured within protodunes match those often attributed to sandsheets (Fryberger et al., 1979; Kocurek and Neilson, 1986; Chan, 1989). Processes operating on protodunes surfaces generate low- to moderate-angle wind-ripple and small-scale cross-stratification, discontinuous coarse-grain lag deposits, preserved ripple forms supported by finer grains (similar to Fryberger et al.'s (1992) 'poured-in texture'), and 10 cm thick wind-ripple sets, all sedimentary features previously attributed to sandsheets (Fryberger et al., 1979; Loope, 1845, 1985; Kocurek and Neilson, 1986; Chan, 1989; Condon, 1997). For these reasons we hypothesize similar subsurface stratigraphic features previously attributed primarily to sandsheet deposits may also record protodune stratigraphy.

Dune genesis

From the observations and interpretations presented here, it seems apparent that protodunes and their internal stratigraphy grow in a defined and order progression from flat nucleation sand patches to slightly higher relief mature protodunes with moderate-angled lee slopes, low- to moderate-angled internal stratigraphy and pronounced bedform asymmetry, before dunes develop with high-angle stratigraphy. This observation is in line with more modern understanding of autogenic sedimentary transport processes birthed out of Bagnold's (1941) earliest works noting slipfaced dunes only originate above a minimum length, dependent on grain size. Recognizing the linked dependency between slipface development and grains in transport helped more recent

authors develop a theory of dune genesis dependent on sand flux (q), wind friction speed (or basal shear velocity often represented as u^*), and saturation distance of the sand flux (L_{sat}) (Kroy et al., 2002; Andreotti and Claudin, 2007; Parteli et al., 2007). Kroy et al. (2002), Parteli et al. (2007) and Andreotti et al., (2010) all report that decreasing average grain size decreases the grain inertia needed for transport, decreasing the flow saturation length (L_{sat}). L_{sat} in turn scales with the maximum critical size for transient protodunes, nucleating as a small wind-rippled sand patches, before they develop into slipfaced dunes (Kocurek et al., 1992; Momiji et al., 2002; Kroy et al., 2002; Andreotti and Claudin, 2007; Parteli et al., 2007; Andreotti et al., 2010).

This critical size for dune growth, dependent on the grain size characteristics, wind speeds, and lagged sand flux at White Sands Dune Field, is captured atop the first surveyed dune's crestline within the time series topographic overlay (Fig. 10b). As early as the June, 2008 we see the growth of a secondary protodune from an initially well-developed asymmetric protodune present in the June, 2007 topographic data, with obvious distinction between the two protodunes in January, 2009 (Fig. 10b**)**. Sometime after the after the June, 2010 survey and before the November, 2015 survey, preservation of progradational, high-angle dune stratigraphy indicates this spawned protodune develops a permanent slipface. Field observations report a considerable median grain size decrease from 8.8 mm in diameter on the relict wind-rippled protodune atop the first surveyed dune to 5.5 mm in diameter comprising the spawned protodune/dune's crest. The spawned dunes well-developed asymmetric crest, prone to advanced flow expansion, may act as a more efficient sand trap than the relict protodunes less

developed, less asymmetric crest, possibly explaining this spatial gain sorting (Nielson and Kocurek, 1986; Kocurek et al., 1992). As transporting winds partition lower medium- to fine-grains from the relict protodune they are perhaps preferentially trapped on the spawned protodune's lee slope, and build to a high-angle behind a more developed crest. This natural grain fractionation process most likely promotes permanent slipface development within the increasingly finer-grained, spawned protodune while inhibiting slipface growth in the relict protodunes.

Before reaching this critical protodune size, the initially well-developed protodune's topographies align with successively steepening low-moderate angled stratigraphic packages bound by first order bounding surfaces (Fig. 10 b) within the first dunes stoss slope (Fig. 6 #5). Here we interpret this aggradation stacking pattern not seen in any upwind migratory protodunes as a the most developed protodunes response to some natural sediment flux "traffic jam," where near surface flow conditions no longer favor rapid migration and instead favor increasing protodune size by merging of protodunes. This aggradation increases bedform height and creates a sufficiently sheltered lee slope which appears necessary for the final protodune growth stages. As advanced flow expansion and eventual flow separation trap fine grains from advecting downwind, the protodune's critical size decreases corresponding to the bedforms decreasing mean grain size, leading to permanent slipface development.

Summary

In conclusion, the low-angle stratigraphy deposited within the White Sands Dune Field's undulatory, low-relief, upwind margin sandsheet is protodune stratigraphy.

Although the low-relief, marginal area Fryberger et al. (1979) designates as ‘sandsheet’ is covered with thin patches of transitory sand, once migration commences in a net positive sand supply, protodune initiation and growth takes over. Incipient migrating sand patch features only a few cm high may account for some flat-lying wind-ripple stratification imaged along the upwind transect, but as stated previously their flat lying morphologies would not exert much flow modification on the transporting wind and therefor initiate little sand deposition. Additionally, from our observations these features only existed temporarily on the scale of days, migrating short distances and could not account for wide-spread low angle reflections seen in the data. Only when significant protodune growth commences generating more permanent migrating bedforms with substantive leeward flow separation driving deposition can extensive flat-lying to moderate-angle stratigraphy marked by coarse grained lag structures, fine-grained supported coarser ripple forms, as well as sporadic small-scale cross-bedding within more common planar wind-ripple stratification accumulate. This stratigraphy marks the passage of bedforms spatially marginal to and temporally before high-angle dune stratigraphy.

CHAPTER III

LOW-ANGLE STRATIFICATION IN ANCIENT EOLIANITES

Low-angle, wind-blown stratification within ancient eolian systems often is interpreted as sandsheet deposits (Loope, 1984, 1985; Chan and Kocurek, 1988; Chan, 1989; Mountney, 2006; Jordan and Mountney, 2010; Lawton et al., 2015). Previous studies attribute wide ranges in grain sizes and bed thicknesses to sandsheet deposition without directly linking the morphodynamics of the geomorphic form that created the stratigraphy or drawing a connection between low- and high-angle eolian strata. Here we develop a process-based model for the accumulation of low-angle strata in ancient eolian systems, and discuss several factors influencing low-angle preservation.

Eolian Sediments of the Cutler Group, Southeast Utah

The late Paleozoic Permian Cutler Group, approximately 2000 ft. within the study area around Canyonlands National Park, represent the final stages of deposition within the Paradox foreland basin of southeast Utah in which sediment filled and overstepped the Paradox Basin's forebulge, transitioning the basin from an under-filled to over-filled basin (Loope, 1984; Condon, 1997; Barbeau, 2003). Complex interactions and abrupt facies variability occur between eolian, marine and fluvial strata that define the late stage basin fill and also represent sedimentary responses to eustatic, climactic and tectonic controls (Loope, 1984; Blakey, 1988; Condon, 1997). The eolian units in the informal lower Cutler, and the White Rim and Cedar Mesa formation sandstones represent ergs which were likely sensitive to external forcing factors influencing

sediment accumulation and preservation. Long-term tectonic subsidence related to the load emplacement of the Uncompahgre uplift was likely the greatest factor in preserving the thick succession of eolian sequences in the area (Kluth and Coney, 1981; Ye et al., 1996; Nuccio and Condon, 1996; Howell and Mountney, 1997; Dickinson and Lawton, 2003; Soreghan G.S. et al., 2012). However, glacio-eustatic cycles linked to long-orbital Milankovitch cyclicity are thought to be the main driver of accumulating eolian sediments of the lower Cutler Group, Cedar Mesa and White Rim Sandstones (Loope, 1985; Dickinson et al., 1994; Rankey, 1997; Mountney, 2006; Jordan and Mountney, 2010). Brief periods of dune field construction, and accumulation marked the convergence of ideal conditions for eolian processes: strong monsoonal winds, evolving semi-aridity, ice house conditions, and enormous sediment supplies exposed along the western marine margin as well as expanded areal extent for eolian processes during sea level lowstands (Loope, 1985; Chan and Kocurek, 1988; Mountney, 2006; Soreghan G.S. et al., 2008; Jordan and Mountney, 2012; Lawton et al., 2015).

Eolian units of the lower Cutler Formation

Originally named the Rico Formation (McKnight, 1940), the Elephant Canyon Formation, which sits in the eastern Island in the Sky and Needles districts of Canyonlands National Park, Utah (Fig. 11), signifies the prolonged transition between the underlying marine Hermosa Group and overlying continental Cutler Group. The Elephant Canyon Formation intercalates with the overlying Cedar Mesa Sandstone (Baars, 1962). Loope (1984) and Loope et al. (1990) replaced ‘Elephant Canyon’ with the informal term ‘lower Cutler beds’, which is now widely used (c.f., Condon, 1997;

Rankey, 1997; Soreghan M.J. et al., 2002). The lower Cutler beds are composed of carbonates and sandstones interpreted as dune and non-eolian terrestrial facies deposited in a wet-eolian system, in which a water-table rise stabilizes the depositional surface from deflation and allows vertical sediment accumulation (Loope, 1984; Kocurek et al., 1992, 2007; Kocurek and Lancaster, 1999). Flat-bedded sandstones occur throughout the unit and are interpreted as sandsheet deposits (Loope, 1984; Kocurek and Neilson, 1986; Condon, S.M., 2000; Jordan and Mountney, 2010). Jordan and Mountney (2010) interpreted the system as a northwest-southeast trending 5 to 20 km wide coastal dune field exposed primarily in the eastern districts of Canyonlands National Park, Utah (Fig. 11). Dune cross-stratification display a wide range of southeast dip that indicates a dominant transport direction toward the southeast. The dune stratification is thought to reflect regional monsoonal climactic patterns that transport sediment from westerly shore face sediment supplies (Loope, 1984; Peterson, 1988; Jordan and Mountney, 2010).

Cedar Mesa Sandstone

Attaining a thickness greater than 1000 m in the Circle Cliffs Trough of south central Utah, the Permian (Wolfcampian) Cedar Mesa Sandstone represents accumulation in dominantly dry erg-center, and marginally wet coastal eolian systems (Langford and Chan, 1993; Condon, 1997; Mountney and Jagger, 2004; Mountney, 2006). Dre-eolian systems record winds saturated with sediment undergoing downwind downstream deceleration, here due to flow expansion into a topographic basin, reducing sediment transport capacity and driving deposition opposed to continued transport or

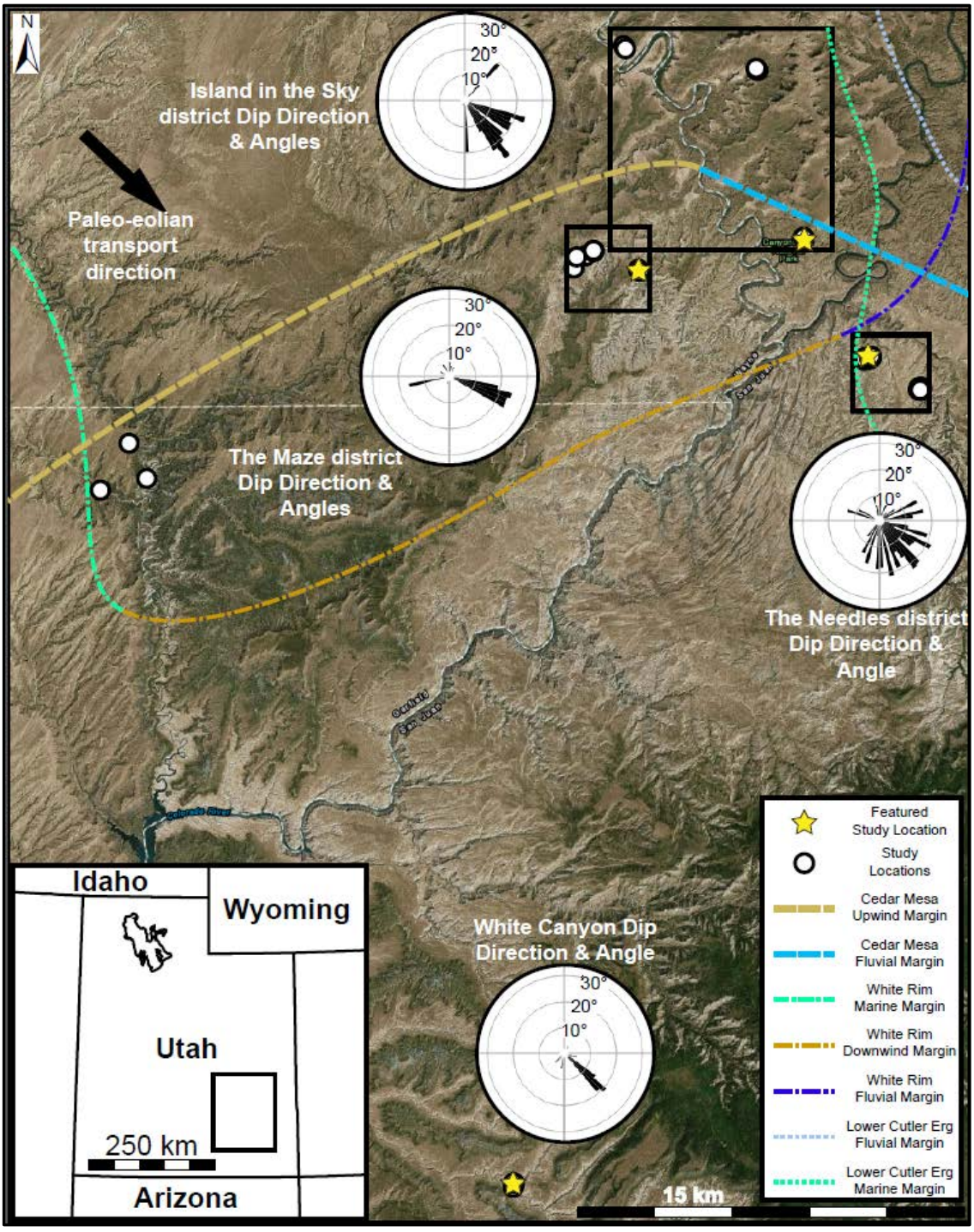

Figure 11. Study locations from field campaign in southeast Utah. Note generalized dune field margins for the Cedar Mesa Erg, White Rim Erg, and lower Cutler Formation Erg modified from Langford and Chan (1993), Chan (1989), and Jordan and Mountney (2010). Paleo-eolian transport direction is taken from these authors as well as collected dip angles throughout our study.

deflation (Kocurek et al., 1992; Mountney and Jagger, 2004; Mountney, 2006). The Cedar Mesa dune seas margins remained relatively stable through time, and any facies variation within the unit corresponds to spatial rather than temporal changes (Langford and Chan, 1993). At the upwind marine margins parallel to the paleoshoreline and downwind fluvial dominated margins perpendicular to Uncompahgre sourced fluvial systems (Fig. 11), water-table fluctuations linked to sea level changes and fluctuating fluvial processes greatly influenced wet-eolian system accumulation, locally limited the extent of eolian processes, and periodically flooded and/or destroyed the dune field at various scales (Blakey, 1988; Blakey et al., 1988; Peterson, 1988; Langford and Chan, 1993; Mountney and Jagger, 2004). Downwind margin sediments show increasing frequency of surfaces marking fluvial flooding and dune field erosion as well as more abundant smaller bedforms and wide inter-dune deposits (Langford and Chan, 1993; Mountney and Jagger, 2004). Flat-bedded sandstone, dune and non-eolian terrestrial facies assemblages make up to 90 percent of sediments within the Cedar Mesa Sandstone (Loope, 1984, 1985; Condon1997; Mountney, 2006). Lenticular beds of flat–lying to low-angle wind-ripple laminae and small-scale cross-strata are most prevalent at dune field margins where they almost always overlie deflation surfaces at the base of erg sequences (Loope, 1984; Langford and Chan, 1993; Condon, 1997; Mountney and Jagger, 2004). Dune facies cross-beds possess a southeast dip, and cross-bed set thickness and grain size decrease from the northwest to the southeast suggesting a dominant northwestern wind direction as well as decreasing transport capacity downwind (Loope, 1984; Langford and Chan 1993; Condon, 1997; Mountney, 2006).

White Rim Sandstone

The 60 to 250 m thick Permian (Leonardian) White Rim Sandstone is interpreted as a seasonally wet coastal dune field intermittently flooded by marine waters during a peri-glacial climate (Blakey et al., 1988 Condon, 1997; Soreghan M.J. et al., 2002; Lawton et al., 2015). The Toroweap Sea and Kaibab Arch to the west and southwest demarcate complex shoreline facies transitions to marine carbonate and sandstone (Fig. 11) and indicate close proximity to interaction with marine environments (Blakely et al., 1988; Condon, 1997). Flat-bedded sediments previously interpreted as sandsheet facies deposits make up a significant portion of the White Rim Sandstone's basal section and thicken towards the western upwind margin (Chan, 1989). Since these deposits attain greatest thickness where eolian deposition begins and thin towards the downwind direction, Chan (1989) hypothesized theses sediments represent the progradational downwind leading edge to the main erg system as a precursor to main erg accumulation. Dominantly northwesterly winds transported massive amounts of sand to the dune field from western shore face sediment caches, whereas subordinate modified trade winds proximal to the Uncompahgre uplift delivered less common continentally derived sediments (Kaloma and Chan, 1988; Lawton et al., 2015).

Methods

Data was collected around Canyonlands National Park in Utah (Fig. 11) during the summer of 2016 using Giga-Pan photomosaics and vertical hand measured stratigraphic sections. Data collected documented the occurrence and frequency of low angle stratification within the Cedar Mesa Sandstone, White Rim Sandstone, and lower

Cutler Formation's eolian units for comparison to the stratification documented by GPR at White Sands. We targeted the erg center and downwind margin of the Permian White Rim sandstone as an example of a wet-eolian system and the upwind margin, dune field interior and downwind margin of the Permian Cedar Mesa Sandstone, serving as an example of a dry-eolian system in specific localities while showing wet-eolian characteristics in other localities. We also focused on the upwind, upper eolianite members of the informal lower Cutler Group/Elephant Canyon Formation/Rico Formation, a typical wet-eolian system.

Giga-Pan photomosaics correspond to several field sites around Canyonlands National Park recorded by Loope (1984, 1985), Chan and Kocurek (1988), Chan (1989), and Mountney (2006) which demonstrate low-angle stratigraphy preservation. At each field site, typically 3 vertical sections were measured at approximately 30 m intervals, depending on outcrop accessibility and exposure, and hand sample identifications of the grain type, grain size, texture and stratigraphy were recorded. All grain metrics were recorded in the field through visual inspection. Dip and dip direction of the stratification were recorded using a Brunton compass. This level of analysis was sufficient for the focus of this investigation, which is on the stratigraphic architecture.

Outcrops were photographed from various angles with high resolution Giga-Pan photogrammetry to capture a comprehensive 3-dimensional outcrop expression. Photo-mosaics constructed from the high-resolution images provide additional support to hand measured observations while constructing schematic outcrop representation. This type of documentation allows for comparison between the frequency, extent and nature of flat

lying and low-angle protodune stratigraphy observed in the rock record to that interpreted within the previously collected GPR transect.

Sedimentary Facies

The outcrop studied reflect various types and degrees of sedimentary processes at the time of deposition. The major facies identified in this study were: 1) horizontal to low-angle, mm scale laminations, 2) low- to moderate-angle, ~10 cm thick laminae sets, 3) dune-scale, high-angle cross-bedding, and 4) muddy/silty to very fine-grained, poorly stratified/unstratified sediments (Table 2).

Measured Sections

In order to effectively assess the occurrence and nature of low angle stratification within eolian successions we visited 14 different study areas corresponding to reports of 'sandsheet' within the White Rim Sandstone, Cedar Mesa Sandstone, and eolian units of the lower Cutler Formation by Loope (1984, 1985), Chan and Kocurek (1988), Chan (1989), and Mountney (2006). Of these visited sites, several proved unsuitable for investigation due to sheer cliff forming nature of these rock units. Other sites, especially those targeting the Cedar Mesa sandstone along the Dirty Devil River near Poison Spring Wash and within North Hose Canyon of Canyonlands National Park's The Maze district, did not show any low angle stratification at all despite previous work suggesting these areas were sandsheets. From the sites displaying low angle stratification suitable for safe investigation 20 measured vertical sections were collected along with corresponding photomosaics. 176 dip measurements were collected throughout this study, 52 were of apparent dips due to the lack of exposed bedding planes for more

Facies:	Description:
Horizontal to low-angle, mm-scale laminations	Poorly-sorted medium- to fine-grained sandstone (Fig. 12a); rare granules and coarse-grains (Fig. 12b); bimodal coarse-grained lag rarely form continuous stringers, arranged in single grain high rows, a few grains long, along lamina surfaces; parallel wind-ripple laminations traceable up to 3 m locally truncate underlying laminations at low angles (<5°); no through going lamina set surfaces; grain sizes change gradationally vertically and horizontally; burrowing only occurs when facies bound by a deflation surface or non-eolian sediments.
Low- to moderate-angle, ~10 cm thick laminae sets	Bimodally sorted granules/coarse-grains and lower medium to fine-grains (Fig. 12c); Continuous lenses of granules and coarse-grain lag traceable from a few 10's of cm to a meter, parallel to horizontal mm scale laminations; abundant wind-ripple laminations; rare preserved wind-ripple foresets; sparse grainfall laminations; ~10 cm thick subparallel laminae sets traceable a few meters truncate underlying sets , which creates low-to moderate-angle scour surfaces; burrowing only documented when facies bound by unit-wide super surfaces interpreted by Mountney and Jagger (2004).
Dune-scale, high-angle cross-bedding	Well-sorted, fine- to medium-sand grains; mm-thick wind-ripple and cm- thick inversely graded grainflow laminations; high-angle trough cross-beds range from 10's of cm to several m thick (fig. 12d); cross-beds range from 1 m to up to 10's of m wide; scour into underlying strata at high angles, 0.5 to 1 m deep depending on overlying set size; moderate- to high-angle reactivation surfaces cut across bedding; high-angle foresets grade downwards to low-angle wind-ripple laminations, contain rare coarse-grains especially if proximal to dune field margins; 3-Dimensional examination of outcrop confirms if foreset toe steepens into higher-angle strata or remains low-angle; bioturbation and root mottling occurs in facies' most upper portions, can impart a massive appearance.
Muddy/silty to very fine-grained, poorly stratified/unstratified non-aeolian sediments	Much more recessive than adjacent sandstone beds; bound repetitive eolian facies successions bases and tops (Fig. 12e); clay-sized, silt-sized, and very-fine sand grains; carbonate cementation, and 1 to 5 cm diameter carbonate nodules are common; rare angular clasts did not effervesce or dissolve in dilute hydrochloric acid, and matched physical appearance, hardness and crystal habit of orthorhombic anhydrite and monoclinic selenite (Fig. 12f); often heavily bioturbated; sand grains and carbonate cementation fill burrows, extend into underlying sandstone beds; overlying sandstones frequently scour into this facies and can completely remove its total thickness.

Table 2. Sedimentary facies encountered during data collection.

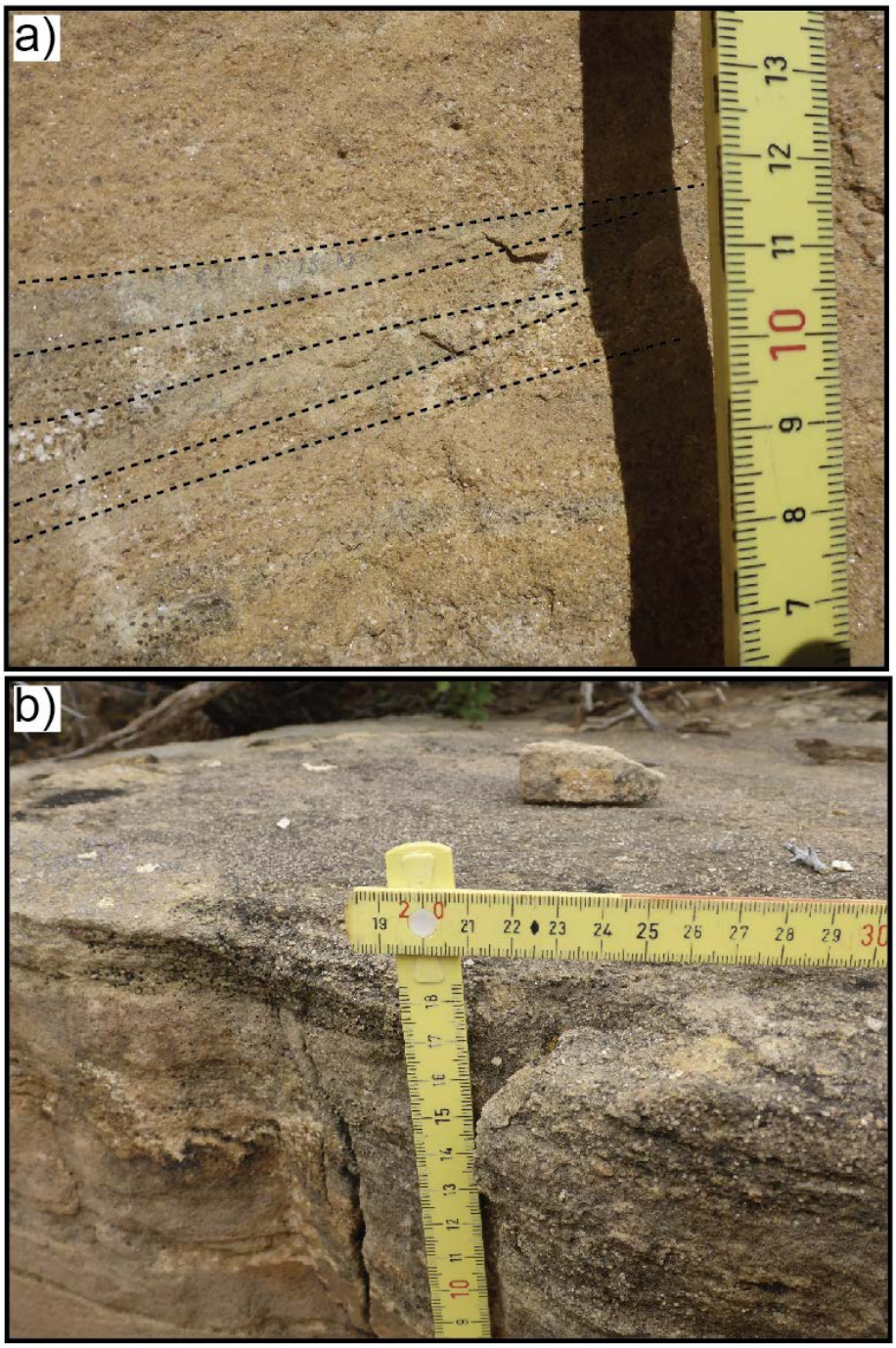

Figure 12. Representative sedimentary facies within investigated eolian successions. (a) Bimodally sorted, mm scale laminations (outlined with stippled lines) trucating underlying strata at low- to moderate-anlges. (b) Coarse-grains dominating mm scale, flat-lying wind-ripple stratification. (c) Low-angle, ~10 cm thick sets. Note local sour into underlying strata directly above measuring tape. (d) High-angle dune cross-bedding forming 1-2 m thick sets. (e) Silty, poorly stratified non-eolian sediments marking deflation surface between two eolian successions. (f) Evaporite clasts at the base of an eolian succession.

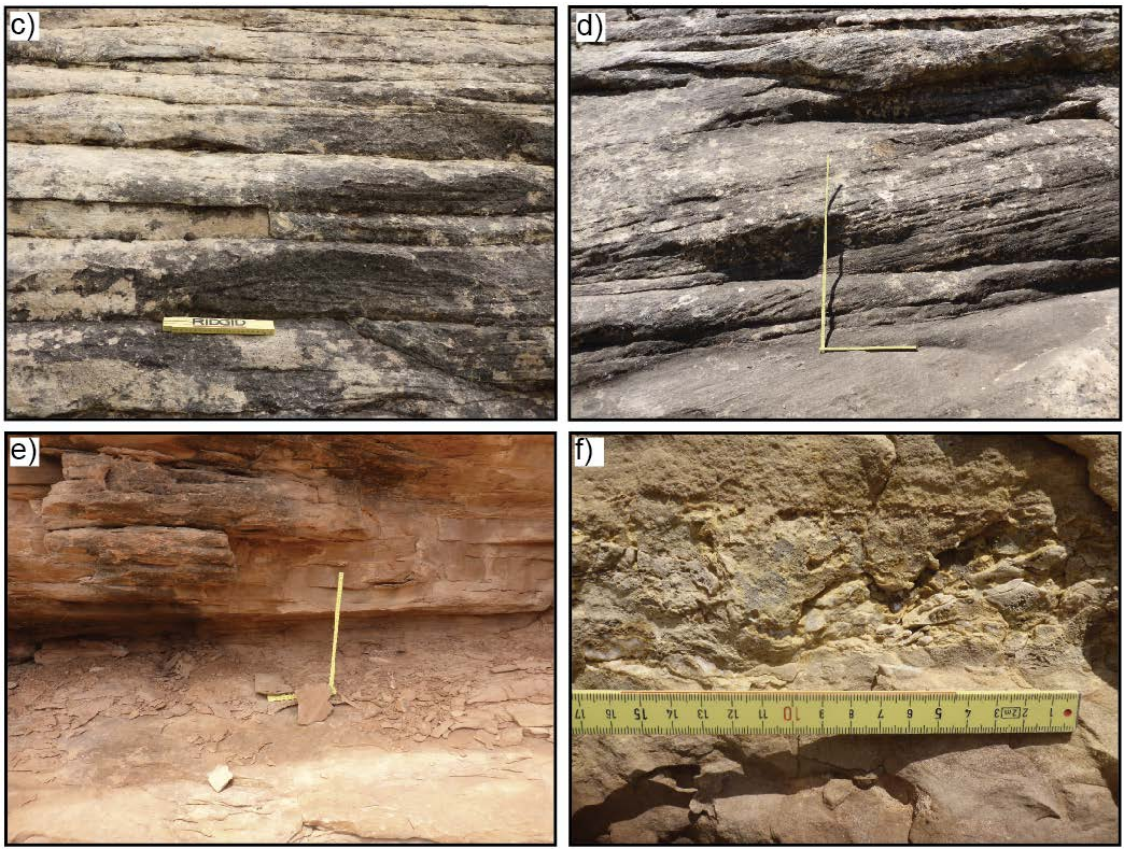

Figure 12 Continued.

accurate dip/dip direction measurement. These measurements focused primarily on the low- to moderate-angle stratigraphy exposed at each outcrop. The lower-angled measurements total reported frequency compared to higher-angle measurement frequency collected along abundant, well exposed, steeply dipping cross-trough bedding lending themselves to much easier, accurate measurements, does not reflect the frequency of the various stratigraphic features encountered throughout this study. Here we present 4 sites at Big Spring Canyon, The Maze Overlook, White Canyon, and White Crack Overlook that most clearly show the different nature at which low-angle

stratigraphy is expressed within the rock record (Table 3). A legend for all symbols used in figures 14-17 is shown below in figure 13.

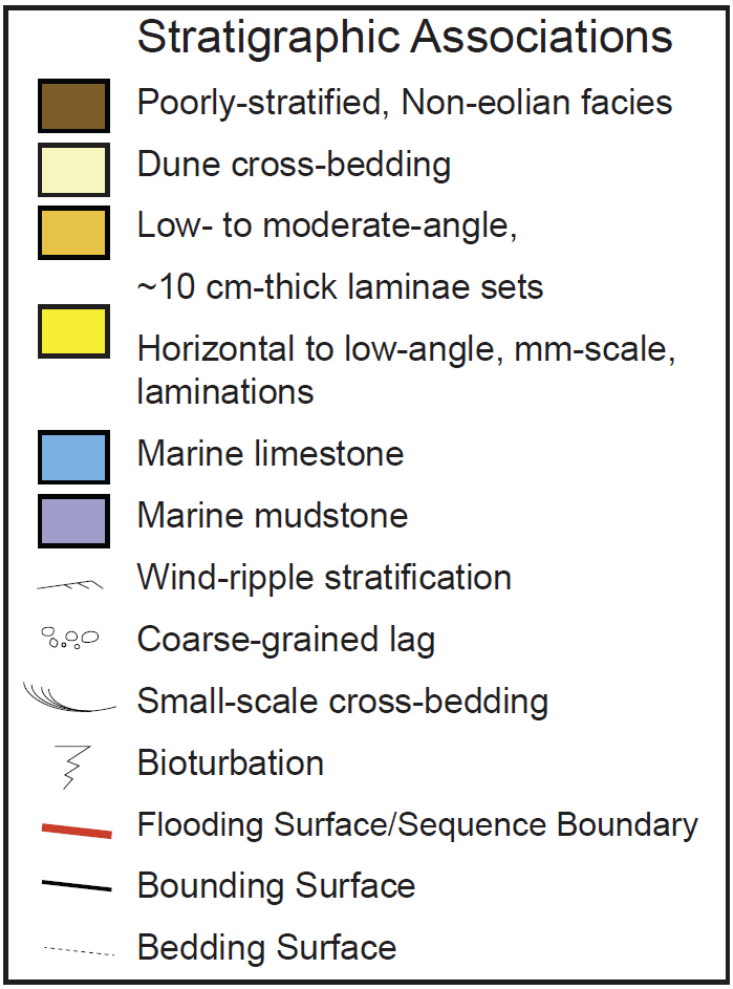

Figure 13. Legend for figures 14-17.

Study Location:	**Description:**	**Sedimentary Facies:**	**Interpretation:**
Big Spring Canyon (Fig. 14)	The Needles district of Canyonlands National Park; repetitive marine/non-marine/aeolian sequences at the lower Cutler Formation's near shore, wet-eolian system, upwind, nearshore margin (Loope, 1984; Jordan and Mountney, 2010, 2012).	▪Horizontal, mm-scale laminated facies overlies shore face sandstone beds and marine sediments ▪Low- to moderate-angle facies erosionally scours into underlying mm-scale sediments with shallow-wavy erosional contact ▪Mm-scale sandstone facies and clay rich non-eolian facies sediments overly low- to moderate-angle facies sediments, downward burrowing and mud cracks ▪Moderate-angle, ~10 cm-thick beds overly and completely replace mudstones locally ▪Small-scale cross-bedded dune faces erosionally scours ~10 cm thick beds ▪Cross-beds increase thickness from 0.5 to 3-4 m ▪Clay-rich non-eolian facies with mud cracks overlies dune sediments ▪Small-scale dune facies sets give way to larger sets ▪Uppermost marine sediments truncate dune stratigraphy.	▪ Sand patches, and early protodunes migrating very proximal to receding shoreline deposit basal-most terrestrial sediments ▪ Protodunes increase in size and lee slope development while continuing to deposit sediment ▪ Transition to low-energy wet/lagoonal, back to arid environments ▪ Resumed eolian processes driving protodune and dune growth and deposition ▪ Dune field deflates to lower energy mudstone depositional setting, and dries to resume eolian dune accumulation ▪ Marine incursion drowns dune field signifying a new sequence.
The Maze Overlook (Fig. 15)	The Maze district of Canyonlands National Park; White Rim Sandstone's wet-eolian system erg center facies.	▪Basal ~10 cm-thick sets with occasional small-scale cross-beds about 1 m wide ▪Isolated dune facies sediments scours into underlying ~10 cm-thick sets, pinches out at high angles ▪Flat-lying, exceptionally coarse grained, mm-scale facies sediments onlap and cover dune sediments ▪Overriding dune sediments bound flat-lying sediments with planar, irregular or wavy erosional contacts, eventually replacing all eolian sediments gradually along the outcrop ▪Uppermost dune sediments burrowed and display signs of marine reworking of dune topography.	▪ Advanced stage protodunes with developed crest lines with advanced flow expansion deposit first preserved eolian sediments ▪ Isolated dunes develop ▪ Conditions favorable to low-angle accumulation take over; low profile protodunes deposit coarse-grain enriched sediments ▪ Return to conditions favoring dune deposition return ▪ Upper sequence boundary detected by sedimentary features common to marine flooding.

Table 3. Descriptions of study locations during data collection.

Study Location:	Description:	Sedimentary Facies:	Interpretation:
White Canyon (Fig. 16)	White Canyon near mile 75 of Highway 95, San Juan Co., Utah; Cedar Mesa Sandstone's dry-eolian system erg center (Langford and Chan, 1993); opposite photographed canyon wall due to cliff-like nature.	▪ High-amplitude, wavy, erosional contact separates meter scale dune facies sediments and underlying red to buff, non-aeolian sediments ▪ Low- to moderate-angle ~10 cm-thick occasionally cross-bedded sets overly and onlap 6-8 m thick dune facies compound sets ▪ Small-scale dune facies sediments overlie ~10 cm-thick sets ▪ Upper-most red to buff, intensely burrowed/massive dune facies sediments give way to red to buff non-eolian sediments ▪ All eolian sediments here are unimodal, well-sorted, lower medium- to fine-grained sands.	▪ Well-developed dunes are first preserved sediments within erg growth sequence above non-eolian sediments ▪ High amplitude erosional scour may explain the absence of preserved basal low-angle stratigraphy ▪ Conditions changed to favor local accumulation from very mature protodunes on the verge of dune growth, without destroying dune topography ▪ Onlapping relationship suggests dunes not deflated by decreasing sediment flux and/or cannibalizing, winds ▪ Conditions favorable for dune accumulation resume until dune field deflates and non-aeolian sediments mark the sequence boundary (Loope, 1984, 1985; Mountney and Jagger, 2004; Mountney, 2006).
White Crack Overlook (Fig. 17)	Island in the Sky district of Canyonlands National Park; White Rim Sandstone's wet-aeolian system downwind, fluvially dominated margin (Chan, 1989; Condon, 1997; Lawton et al, 2015).	▪ Basal non-eolian facies contains irregular anhydrite and selenite crystals ▪ Flat-lying mm-scale facies sediments conformably overly the basal non-aeolian sediments ▪ Above a 1 cm thick lamination of enhanced cementation coarse grains appear, gradually increasing in frequency and continuity ▪ Small, shallow channel structure filled with coarse-sand and cobble-sized channel lag pinches into a bounding surface underlying well-sorted, ~10 cm-thick sets ▪ Abundant coarse grains reappear above another through-going bounding surface, decreasing in frequency upward, small-scale cross-bedding increases upwards, set thickness decreases upwards to 1 to 2 cm thick ▪ Dune facies sediments sharply overly low-angle sets	▪ Sabkha-deposits form during drying from underlying Organ Rock's Formations humid environment ▪ Incipient sand patches deposit flat-lying strata from fine-sands trapped on depositional surface connected to fluvially influenced water table ▪ Ephemeral stream channels deliver abundant coarse grains to low-relief bedforms ▪ Natural grain sorting occurs during growth of, and deposition from intermediate protodunes ▪ Advancing progradational erg margin arrives (Chan. 1989) with more poorly-sorted sand supply ▪ Protodune growth drives grain fractionation, crestline and lee-slope evolution and increased flow expansion, while depositing sediment ▪ Dunes grow and accumulate sediment

Table 3. Continued

Figure 14. Schematic representation of the studied Big Spring Canyon eolian succession. (a) Schematic representation of outcrop. (b) Stitched photomosaic of outcrop. Note the perspective of the outcrop resulting from the photomosaic stitching process. Underlying and overlying marine mudstone mark bases of repetitive, eustatic sea level sequences. Thin terrestrial mudstone units mark parasequences-type environmental fluctuations which dictate the accumulation and evolution of eolian bedforms here.

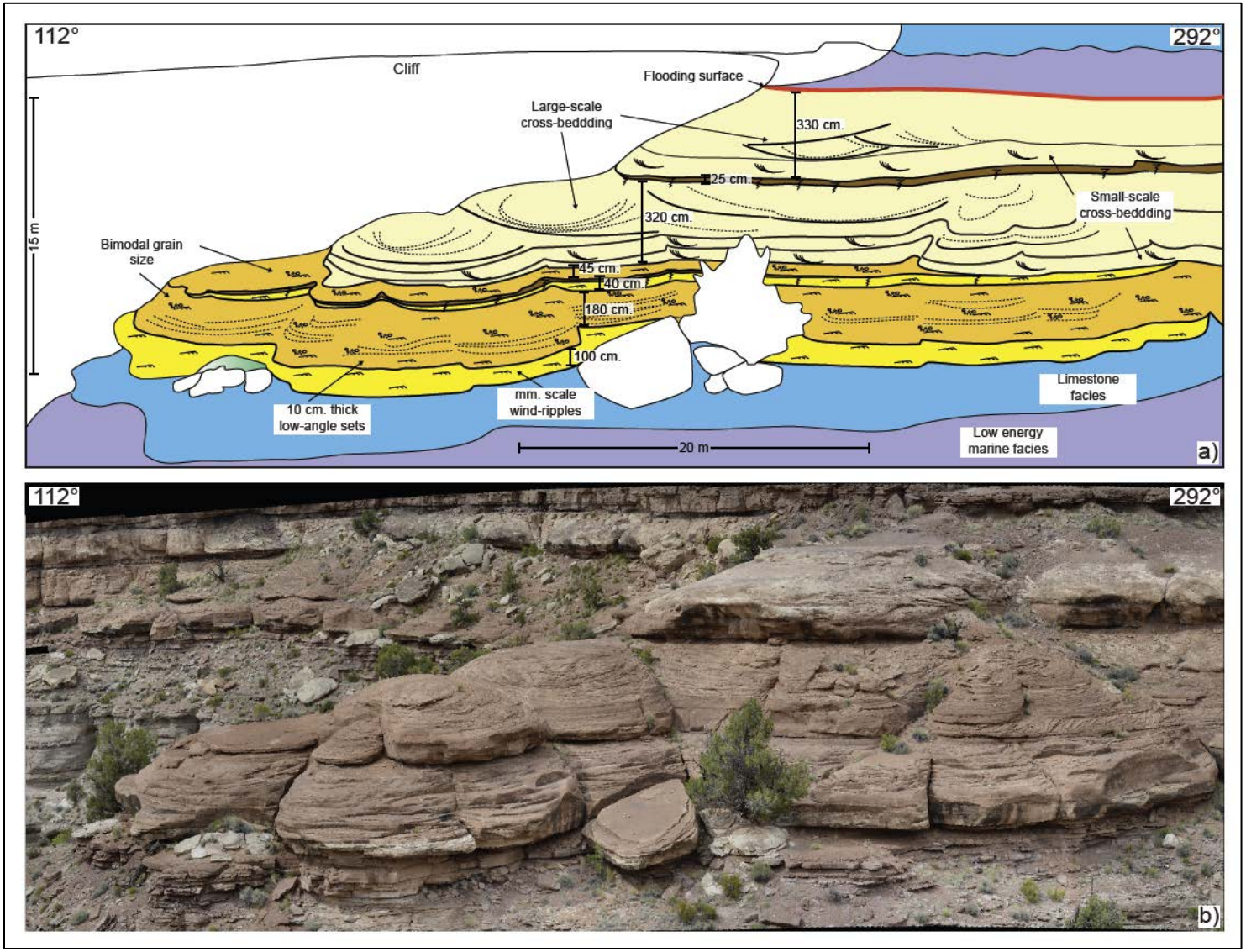
112°
292°
Cliff
Flooding surface
Large-scale
cross-beddding
330 cm.
25 cm.
320 cm.
Small-scale
cross-beddding
15 m
Bimodal grain
size
45 cm.
40 cm.
180 cm.
100 cm.
10 cm. thick
low-angle sets
mm. scale
wind-ripples
Limestone
facies
Low energy
marine facies
20 m
a)
112°
292°
b)

Figure 15. Schematic representation of the studied The Maze Overlook eolian succession. (a) Schematic representation of outcrop. (b) Stitched photomosaic of outcrop. Note the perspective of the outcrop resulting from the photomosaic stitching process. This outcrop is essentially planar, but appears curved due to level of zoom while capturing the photomosaic. Underlying non-eolian, clay-rich, and silty layers represent final sediments within the Organ Rock Formation and are capped by a sequence boundary between overlying eolian White Rim sediments. Isolated dune-cross bedding within more typical protodune stratification indicates bedforms close to the critical conditions for dune growth subjected to various fluctuating conditions.

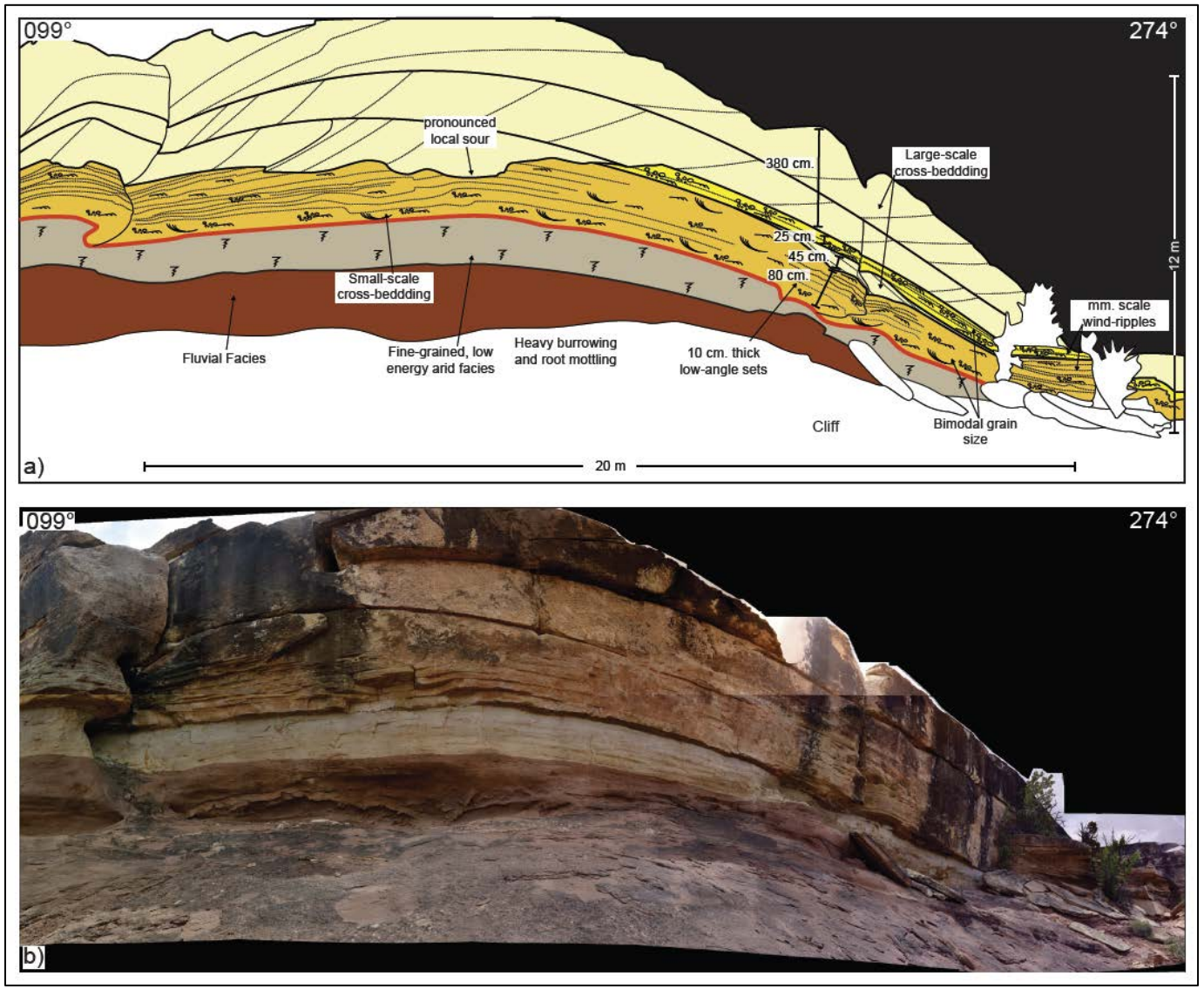
099°
274°
pronounced
local sour
380 cm.
Large-scale
cross-beddding
25 cm.
45 cm.
80 cm.
12 m
Small-scale
cross-beddding
mm. scale
wind-ripples
Fluvial Facies
Fine-grained, low
energy arid facies
Heavy burrowing
and root mottling
10 cm. thick
low-angle sets
Cliff
Bimodal grain
size
a)
20 m
099°
274°
b)

Figure 16. Schematic representation of the studied White Canyon eolian succession. (a) Schematic representation of outcrop. (b) Stitched photomosaic of outcrop. Note the perspective of the outcrop resulting from the photomosaic stitching process. Anomalously thick protodune section within dune cross-bedding dominated erg center environment suggests a departure from normal conditions to those ideal for protodune stratigraphy accumulation and preservation, followed by a fluctuation back to more dune-favoring conditions.

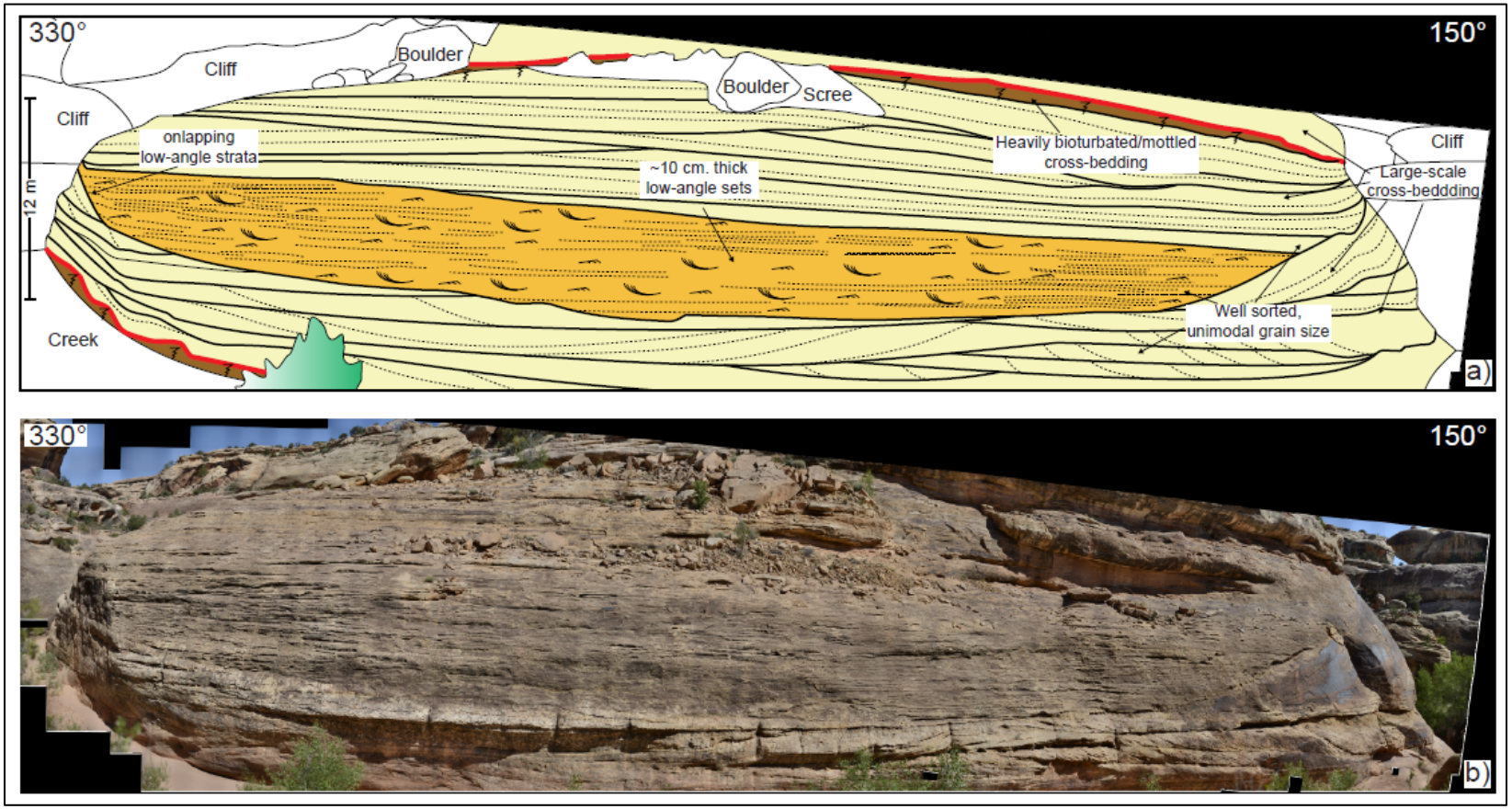
330°
150°
Cliff
Boulder
Boulder
Scree
Cliff
12 m
onlapping
low-angle strata
~10 cm. thick
low-angle sets
Heavily bioturbated/mottled
cross-bedding
Cliff
Large-scale
cross-beddding
Well sorted,
unimodal grain size
Creek
a)
330°
150°
b)

Figure 17. Schematic representation of the studied White Crack Overlook eolian succession. (a) Schematic representation of outcrop. (b) Stitched photomosaic of outcrop. Note the perspective of the outcrop resulting from the photomosaic stitching process. This outcrop is slightly curved towards the west and a sheer cliff forms to the bottom left (west) of the illustrated image which enhances the distortion due to the level of zoom used to capture images. Thicknesses are essentially preserved across the outcrop, marked by the measurements in the illustration. Here alternating characteristics within flat-lying, and low- to moderate-angled stratigraphy reflect various conditions which favor uncommonly thick sections of preserved protodune stratigraphy.

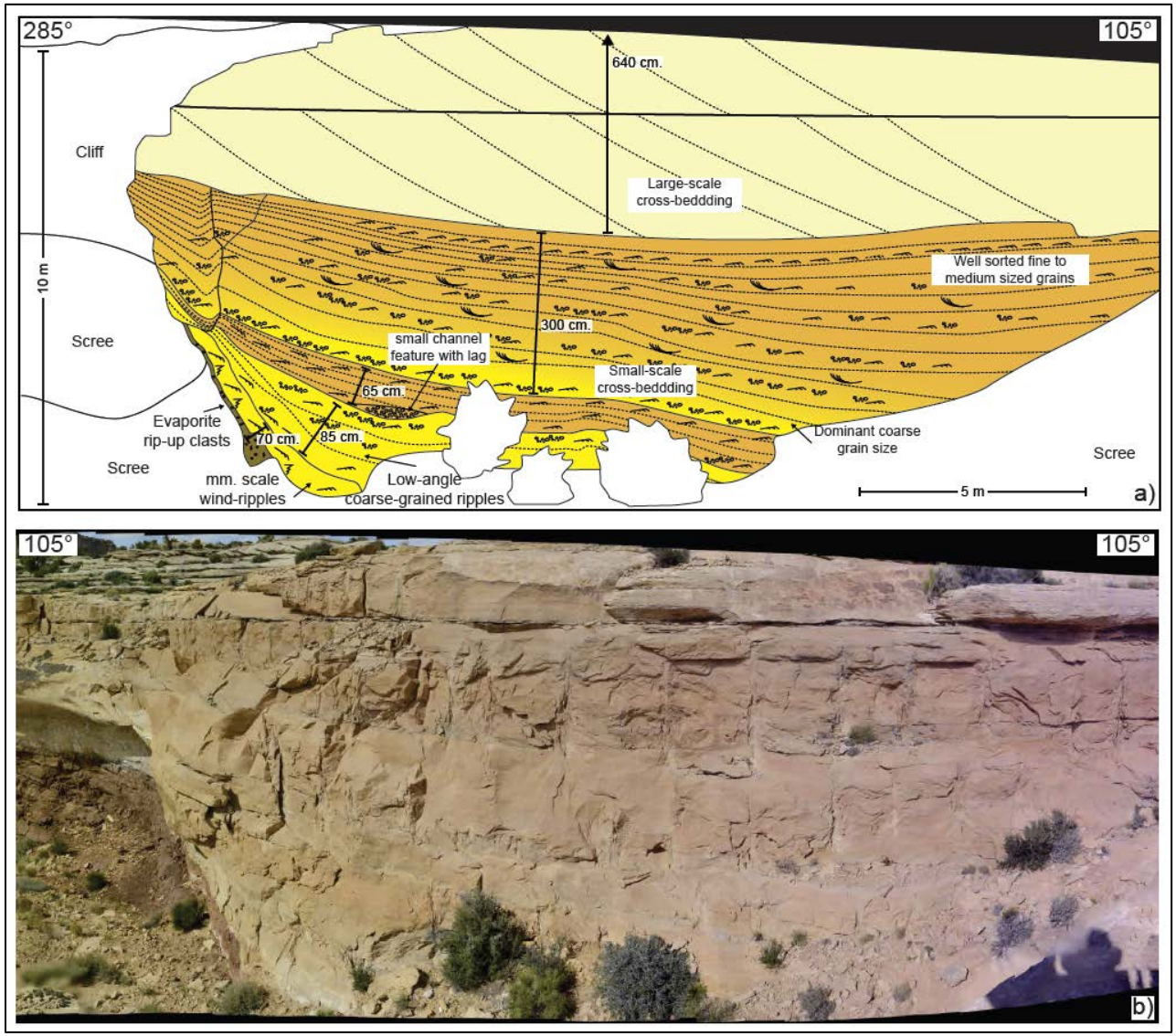
285°
105°
640 cm.
Cliff
Large-scale
cross-beddding
10 m
Well sorted fine to
medium sized grains
300 cm.
Scree
small channel
feature with lag
65 cm.
Small-scale
cross-beddding
Evaporite
rip-up clasts
70 cm.
85 cm.
Dominant coarse
grain size
Scree
Scree
mm. scale
wind-ripples
Low-angle
coarse-grained ripples
5 m
a)
105°
105°
b)

Discussion

The results from the field observations in ancient eolian successions show a predictable vertical successions of facies from nearly flat-lying, to low- and moderate-angle strata, to high-angle dune cross-stratification (Fig. 18). Low-angle eolian strata's typical basal position within eolian successions represents initial stages of eolian accumulation (Mountney and Jagger, 2004). Low-angle eolian bedforms above non-eolian sediments/surfaces, and below dune cross-bedding implies that low-angle bedforms must form as an intermediate stage between non-eolian environments and dune fields (Loope, 1985; Kocurek and Nielson, 1986; Chan, 1989). We find similar relationships and further connect the formation of low angle stratification to the development and migration of protodunes, as with the example at White Sands (Fig. 18). We interpret flat-lying strata as early-stage protodune stratification and low- to moderate-angle strata as intermediate-stage protodune stratification. High angle strata is interpreted as dune stratification that follows the protodunes stages. Additionally we further investigate the preservation of low-angle stratification in the context of the type of eolian system and autogenic processes, such as dune scour, that affect its preservation.

Protodune origins of low-angle stratification

Low-angle, ancient eolian sediments containing coarse-grained lag, occasional high-index ripple foresets, small-scale cross-beds, and rare intercalated high-angle eolian cross-bedding resemble sedimentary features resulting from evolving protodune growth

Figure 18. Typical eolian succession encountered during data collection in southeast Utah. Here we show that geometric and spatial connection between flat-lying ancient eolian strata and early stage protodune stratification, low- to moderate-angle ancient eolian stratification and mature protodune stratification, and high-angle ancient eolian strata and slipfaced dune stratification.

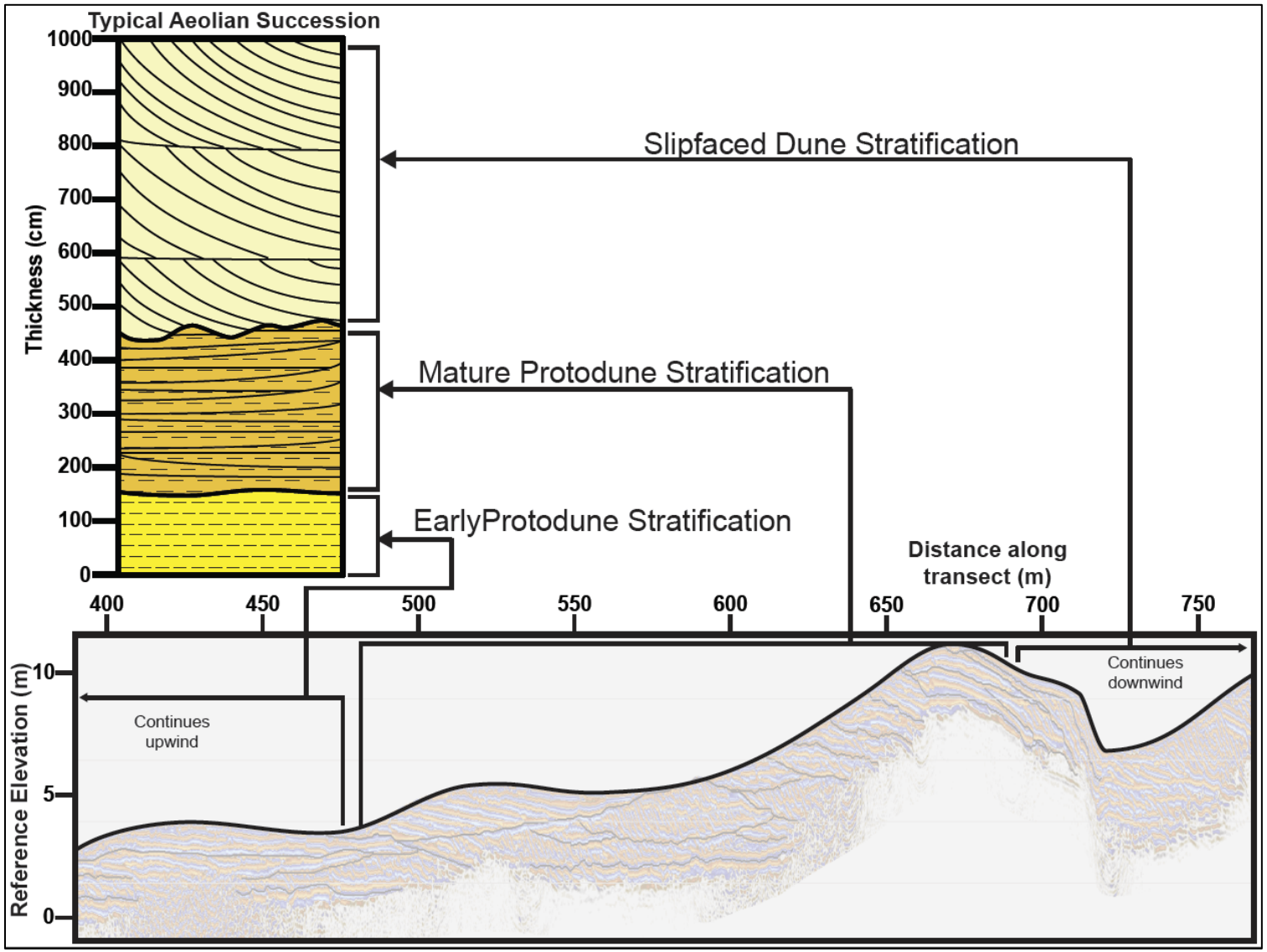
Typical Aeolian Succession
Thickness (cm)
1000
900
800
700
600
500
400
300
200
100
0
Slipfaced Dune Stratification
Mature Protodune Stratification
EarlyProtodune Stratification
Distance along transect (m)
400
450
500
550
600
650
700
750
Reference Elevation (m)
10
5
0
Continues upwind
Continues downwind

documented at White Sands. While previous authors suggest these low- to moderate-angled sedimentary features denote sandsheets, zibars, and granule-ripples (Fryberger et al., 1979, 1992; Loope, 1984; Nielson and Kocurek, 1986; Chan 1989), we add to previous interpretations the possibility that these stratigraphic features correspond to protodune stratigraphy.

Flat-lying (dipping close to 0°), wind-ripple, poorest-sorted sediments, such as those exposed at The Maze Overlook (Fig. 14), most likely correspond to earliest, or lowest relief protodunes. Both the geometry of the stratification and grain size distribution match our previous observations. At White Sands, these types of bedforms developed at the most windward positions in the dune building processes, which temporally would occur at the outset of dune field formation. We thus interpret low-angle stratigraphy as early stage protodunes deposits. Low-angle stratigraphy (greater than 0° and less than 5°), similar to that described at the basal portions of the Big Spring Canyon (Fig. 13) sequence, matches geometries in intermediate protodunes between lowest relief sand patches and slipfaced dunes documented at White Sands. A finer overall grain size population in these sediments as compared to the flat lying sediments likely results from grain sorting processes during bedform growth (Warren, 1971). Well-sorted moderate-angle(between 5° and 15°), small-scale cross-strata less than 1 m wide present at the base of The Maze Overlook (Fig. 14), at White Canyon (Fig. 15), and at the upper portions of the sequence exposed at the White Crack Overlook (Fig. 16) record advanced- stage protodunes with well-developed lee faces. Such strata corresponds to the internal stratigraphy and surface grain sizes we observed for protodunes at the

critical size before forming slipfaced dunes. Additionally, minor low-amplitude scour (less than 5 cm thick) between low- and moderate-angle strata in the rock record correspond to scour recorded between low-relief bedforms reported by Fryberger et al. (1992), and Kocurek et al. (1992) to result from increased leeward flow expansion and turbulent flow responding to lee slope development. This minor erosional scour therefore is an indicator of protodune stratigraphy at an advanced stage.

Erg growth

Low-angle protodune stratification's common basal location within ancient erg successions indicates some correlation between idealized protodune accumulation (Fig. 19), and dune field construction and accumulation phases. Here we use the term dune field construction to represent the confluence of conditions needed for eolian processes and net sand deposition to establish migrating bedforms. During this phase bedforms preferentially migrate and expand sand cover laterally, bypassing accumulation (Wilson, 1971, 1973; Blakey, 1988; Kocurek et al., 1992; Kocurek and Lancaster, 1999). Dune field accumulation alternatively refers to the accumulation surface's vertical rise over time to form a body of strata, (Brookfield, 1977; Kocurek, 1992; Mountney, 2006). In line with these dune field phases, Loope (1985) hypothesized that erg construction, accumulation and deflation cycles are responsible for the Cutler Group's many eolian sequences observed in this study, with construction occurring over a protracted period of time followed by rapid accumulation and deflation. Although Loope's time estimates may not reflect more recent, shorter estimates for the time needed to create dunes and construct ergs, we hypothesize accumulated protodune stratigraphy at the base of eolian

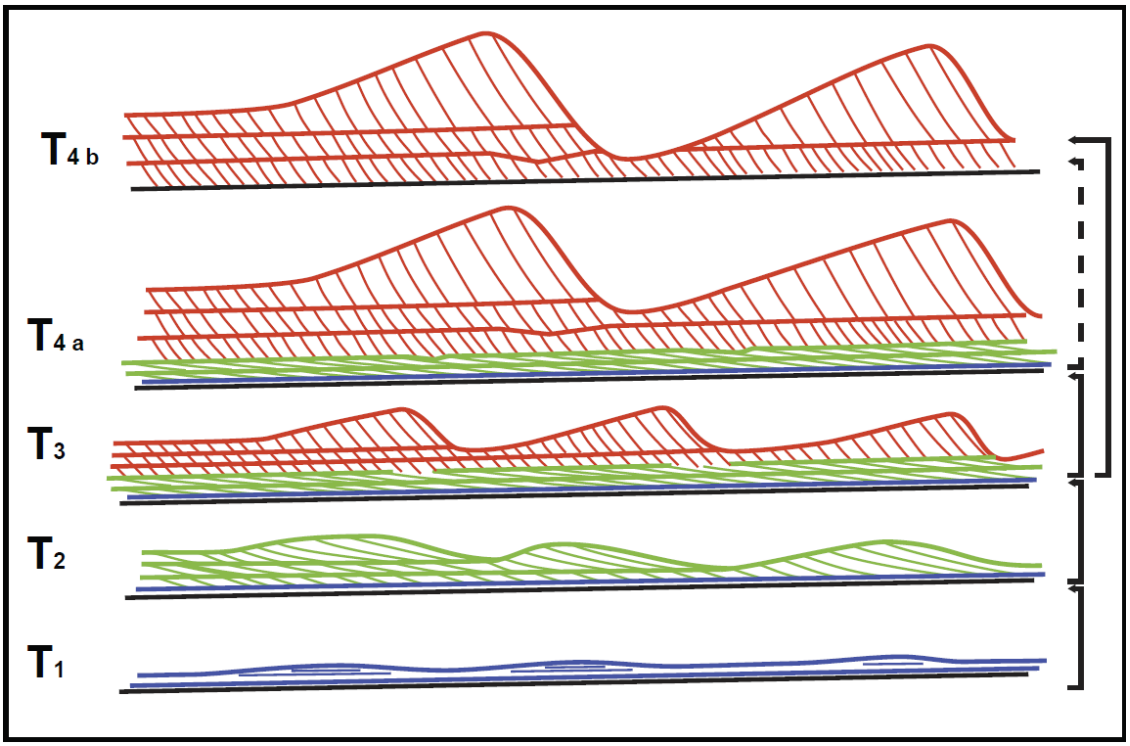

Figure 19. Idealized dune field growth sequence. Base of eolian accumulation sequence is shown in black, flat-lying to low-angle stratigraphy is shown in blue, low- to moderate-angled protodune stratigraphy is shown in green, and high-angle dune stratigraphy is shown in red. Successive time steps occur from T_1 to T_{4a}/T_{4b}, in which a flat bed of sand evolves into mature slipfaced dunes in a manner similar to what we observe in modern eolian environments. This schematic diagram illustrates the process based evolution of eolian bedforms, and the effect that successive bedforms have on underlying stratigraphy. Between T_1 and T_2, wind-rippled protodunes and mature grainfall protodunes grow from incipient sand patches and early protodunes. Between T_2 and T_3, grainfall protodunes accumulate low- to moderate-angle strata and grow into dunes, while leaving some underlying flat-lying to low-angled stratigraphy intact for later preservation. Between T_3 and T_{4a} smaller dunes do not scour away much accumulated protodune stratigraphy while accumulating high-angle dune stratigraphy. More mature, larger dunes grow from these younger dunes. T_{4b} represents a time after T_3 where smaller, younger dunes scour completely through low- to moderate-angle stratigraphy and only preserve underlying lowest-angled strata to none at all, or when larger dunes formed at T_{4a} scoured through high-angled stratigraphy deposited from young, smaller dunes as well as low- to moderate-angle strata accumulated from dunes. If T_{4b} does not follow T_{4a} protodune stratigraphy chances of becoming preserved in the rock record greatly increase.

successions is a hallmark of the transition from construction phases to accumulation phases (e.g. Kocurek et al., 1992; Momiji et al., 2002; Kroy et al., 2002). During this stage low-angled protodunes deposit low-angle strata as they grow into slipfaced dunes

which dominate accumulation phases and therefore account for proportionally more sediment preserved in the rock record (Fig. 18 & 19). In this manner we suggest that low-angle strata must form first before cross-bedded dune facies sediments can accumulate, and therefore protodune stratigraphy naturally should be common below dune facies cross-bedding in preserved eolian successions as their formation is required temporally, as well as spatially, before full dune growth.

Accumulation of low-angle stratification

Accumulation of protodune stratification occurs in the manner in which dune stratification accumulates within the different environmental boundary conditions of wet, dry, and stabilizing systems (Kocurek, 1999). The accumulation thickness is limited by the time and length scale over which a protodune becomes a dune. At White Sands for example, the protodunes became dunes over ~600 m. At the average migration rate of 17 m/year the timescale over which protodunes could accumulate would be 35 years. A maximum thickness of protodune strata, at White Sands, which would occur if the protodunes were vertically climbing, is ~4 m. However, at lower angles of the climb the thickness would be substantially less and given the oft cited 10% accumulation thickness of eolian systems, the maximum thickness would be less than 50cm. Thus, the thick sections of a low-angle stratification observed in Cutler Group in Utah implies that the protodune to dune transition was prolonged. Environmental factors such as irregular wind patterns, near-surface water-table, and coarse grain-armoring can limit the growth of protodunes to dunes, which would promote thicker sections of protodune strata than is expected from a typical protodune to dune transition (Nielson and Kocurek, 1986).

Decreased regularity in wind direction and strength could account for thick, low- to moderate-angled protodune sediments exposed at the White Crack Overlook where dip directions in protodune stratification vary greater than 180° (Fig. 16). Unstable wind conditions inhibit permanent dune slipface formation and can retrograde dune forms into large protodunes (Kocurek et al., 1992). This suggests that variable winds could prolong slipface development and promote the accumulation low-angle stratification.

A high concentration of coarse grains within the 550 cm and 150 cm thick low-angle stratification at the White Crack Overlook (Fig. 16) and the Maze Overlook (Fig. 14) respectively, may record the accumulation of protodunes influenced by coarse grains. At the White Crack Overlook a coarse lag filled channel, interpreted as an ephemeral stream, brought coarse grains into the dune field margin. At The Maze Overlook, a high concentration of coarse grains within the unit overlying and onlapping isolated dune cross-bedding suggests that an immature sediment source. From modern observations of protodunes, only a small concentration coarse grains inhibits slipface development (Bagnold, 1941; Kocurek and Nielson, 1986). One explanation for this is that flow saturation length (L_{sat}) increases with an increased abundance of coarse grains (Kroy, 2002; Parteli et al., 2007; Andreotti and Claudin, 2007). Sorting processes would decrease the saturation length over time and allow dune growth after the concentration falls below a threshold as seen at White Sands. At both White Crack Overlook and at The Maze overlook, high concentrations of coarse grains within low-angle stratified units gave way upward to finer grained protodune stratification and ultimately dune stratification, suggesting sorting processes were at work. The increased abundance of

coarse grains would prolong the protodune phase during which low-angle strata would accumulate.

Damp depositional surface created by a near surface water-table limits sediment availability, which could promote the accumulation of thick low-angle eolian units and explain the observations at Big Spring Canyon Overlook (Fig. 14) and White Crack Overlook (Fig. 17). At Big Spring Canyon, observations indicate a near-surface water-table hydrologically connected to an upwind, proximal shore face, similar to that on Padre Island, Texas documented by Kocurek et al. (1992), stabilizes the depositional surface on which protodunes form (Chan and Kocurek, 1988; Jordan and Mountney, 2010, 2012). At the White Crack Overlook (Fig. 16), a fluvially-connected near surface water-table influenced by fluvial systems dominating the downwind margin most likely stabilizes the depositional surface as well, trapping fine sand transported quickly to the downwind margin as sand patches and protodunes. Wet or damp sand's increased threshold velocity prohibits deflation, limits sediment availability, and favors vertical accumulation (Chepil, 1956; Belly, 1964; Bisal & Hsieh, 1966; Svasek and Terwindt, 1974; Azizov, 1977). Long-lived limits on sediment availability may prolong the protodune phase and promote accumulation of low-angle stratification.

Preservation of protodune stratification

Protodunes are precursors to the development of sand dunes and, all else being equal, protodune stratification should occur in the stratigraphic record associated with dune stratification. However, the presence, absence, and lateral variability of protodune

stratification in our measured suggest scour depth, and position within the field are strong controls on the preservation of protodune stratification.

Scour into underlying sediments by lee-side turbulent flows is a major control on the preservation of bedform cross-stratification (Paola and Borgman, 1992; Leclair and Bridge, 2001). The degree of scour depends on the bedform slope and height. Thus, dunes will scour more than protodunes. As a result basal most flat-lying sediments are preferentially preserved over overlying more mature protodune deposits because mature protodunes have low scour potential and are less likely to erode accumulated early-phase protodune stratification. Additionally, because mature protodunes are the phase prior to dune formation, mature protodune stratification directly underlies dune process, which have high scour potential. Variability in scour depth is limited in wet-aeolian systems, whereas in dry systems variability is greater, thus, in wet systems the potential to preserve low-angle strata is higher (Kocurek et al., 1992, 2007; Mountney and Jagger, 2004; Mountney, 2006; Kocurek and Ewing, 2017). This explains the absence of basal protodune stratification in White Canyon (Fig. 16).

The position of protodunes within the dune field can also affect the preservation potential of protodune stratification. For example, dome dunes, a type of protodune, frequently form downwind of dune fields where dunes are ejected from the dune field and lose sediment as they migrate downwind. In this example, the accumulated low-angle stratification is spatially separated from the dune processes, which allows prolonged accumulation of low-angle strata and thus a potentially thick succession that would be less likely to be scoured by dune processes. This can also explain the

preservation of the moderate-angled stratification, which occurs with mature protodunes, such as at The Maze Overlook (Fig. 15). At the White Crack Overlook (Fig. 17) we think the time between accumulating low-angle strata and the arrival of the White Rim Erg's progradational margin to a far downwind position was enough to begin preserving thick accumulations of low-angle strata. Interestingly, complete preserved eolian successions progressing from thick low- to moderate angled stratification to higher angled dune facies sediments at other downwind fluvial influenced erg margins suggest high preservation potential in these environments compared to other erg positions. Here abundant fluvially introduced coarse-grains, elevated water-tables, and temporal separation from dune processes favor protodune growth, accumulation and preservation over dune growth.

Summary

Near flat-lying to moderate-angle strata represents protodune stratification corresponding to the level of bedform development, and their common position below high-angle dune strata indicates their spatial and temporal role in dune genesis. Irregular wind patterns, low sediment availability, near-surface water-table, and coarse-grain armoring alter sediment transport processes acting on protodunes and favor accumulating protodune strata over dunes strata. In the absence of these factors, the protodunes phase should naturally exist unless otherwise removed by scour, in which case dune accumulation dominates. While evolving process-scale mechanisms produce protodune growth and dune genesis sequences in both wet-and dry-eolian systems, low-angle stratigraphy's preservation potential is higher in wet-systems.

Protodunes occur primarily as features which dominate early erg construction periods and therefore commonly bypass accumulation surfaces while growing into dunes. Accumulated protodune stratigraphy most likely marks the transition to punctuated erg accumulation phases, dominated by dunes depositing high-angle strata, and therefore accounts for proportionally less sediment preserved in the rock record. Mature protodunes do scour into underlying flat-lying, low-angle stratification but to a much lesser degree than do dunes. As a result basal most flat-lying sediments are preferentially preserved compared to mature protodune deposits close to dune processes.

CHAPTER IV

CONCLUSION

Protodunes reflect the onset of dune field formation. In modern systems that are typically observed at the upwind margins of dune field and, where dune field formation was observed, protodunes emerge as a precursor to dune formation (Kocurek et al., 1992; Ping et al., 2014). Low angle stratification in the eolian rock record was well described and its context in the eolian system established, but the connection of low-angle stratification to a defined bedform was missing. We used GPR at the upwind margin of White Sands Dune Field, New Mexico to map the internal structure of protodunes and then used those observations to re-evaluate low-angle stratification within the eolian rock record. Flat-lying to moderate-angle radar reflection data collected along White Sands Dune Field's upwind margins represent stratigraphy within migrating protodunes. Commensurate grain size and stratification dip angle changes occur in a predicable fining and gradually steepening fashion corresponding to advanced levels of protodune development and maturity, resulting from evolving near surface flow conditions involved in protodune growth (Kocurek et al., 1992). Correlation between radar reflections and successive time series topographic datasets establishes as correlation between evolving protodune morphology and increasing internal stratigraphic dip angles. Protodunes increase in maturity until they reach a critical size that drives the transition to dune morphology. This transition is marked by fine-grain fractionation, vertical aggradation of low- to moderate-angle strata due to a sediment

flux “traffic jam,” and dramatically increased depositional slopes yielding a permanent slip face and high-angle internal dune stratigraphy.

The results from the field observations of eolian sediments within the Late Paleozoic Cutler Group show a predictable vertical successions of facies from nearly flat-lying, to low- and moderate-angle strata, to high-angle dune cross-stratification, which represents stratigraphy deposited by protodunes as they grow into dunes. According to our idealized model for protodune growth, deposition and preservation of low-angle strata must form first before cross-bedded dune facies sediments can accumulate. Therefore protodune stratigraphy naturally should be common below dune facies cross-bedding in preserved eolian successions as their accumulation is required temporally, as well as spatially, before full dune growth. Although protodune stratigraphy commonly occupies a predictable basal portion within eolian sequences irregular wind patterns, low sediment availability, near-surface water-table, and coarse grain-armoring present at the time of deposition alter sediment transport processes acting on protodunes and favor accumulating low-angle stratigraphy. While similar sediment transport processes produce protodune growth and dune genesis sequences in both wet- and dry-eolian systems, elevated near-surface water-table within wet-systems greatly increases low-angle stratigraphy’s accumulation and preservation potential. Additionally, dunes cannibalizing intermediary sediments overlying low-angle stratigraphy, and temporal separation from dune processes increases preservation potential for low-angle stratigraphy.

Understanding the autogenic processes involved in sedimentary transport responsible for forming and preserving various stages of protodune stratigraphy explains the occurrence of angle-of-repose stratification versus low-angle strata within the rock record. Our process-based approach presented here provides physical reasoning for identifying and predicting low-angle protodune stratigraphy's vertical occurrence and aerial extent within ancient rocks.

REFERENCES

Ahlbrandt, T.S., 1979, Textural parameters of eolian deposits, *in*: McKee, E.D., ed., A study of Global Sand Seas: Professional Paper U.S. Geologic Survey, v. 1052, p. 21-51.

Allmendinger, R.J., 1971, Preliminary evaluation of the role of the hydrologic cycle in the development of the white sands, White Sands National Monument, New Mexico: Geologic Society of America, Abstracts with Programs, v. 3, p. 231-232.

Allmendinger, R.J., 1972, Hydrologic control over the origin of gypsum at lake Lucero, White Sands National Monument, New Mexico [M.S. thesis] Socorro, New Mexico, New Mexico Institute of Mining and technology, p. 182.

Andreotti, B., and Claudin, P., 2007, Comment on 'Minimal size of a barchan dune': Physical Review, v. 76 063301, p. 1-5.

Andreotti, B., Claudin, P., and Pouliquen et al., 2010, Measurements of the aeolian sand transport saturation length: Geomorphology, v. 123, p. 343-348.

Azizov, A., 1977, Influence of soil moisture on the resistance of soil to wind erosion: Soviet Soil Science, v. 9, p. 105-108.

Bagnold, R.A., 1941, The Physics of Blown Sand and Desert Dunes: London, Chapmann and Hall.

Bagnold, R.A., 1954, The Physics of Blow Sand and Desert Dunes: London, Methuen.

Barbeau, D.L., 2003, A flexural model for the Paradox Basin: Implications for the tectonics of the Ancestral Rocky Mountains: Basin Research, v. 15, p. 97-115.

Baars, D.I., 1962, Permian system of the Colorado Plateau: AAPG Bulletin, v. 46, p. 149-218.

Belly, P.Y., 1964, Sand movement by wind: Technical Memoirs U.S. Army Corps of Engineers Coastal Research Center.

Bisal, F., and Hsieh, J., 1966, Influence of moisture on erodibility of soil by wind: Soil Science, v. 102, p. 143-146.

Blakey, R.C, 1988, Basin tectonics and erg response: Sedimentary Geology, v. 56, p. 127-151.

Blakey, R.C., Peterson, F., Kocurek, G., 1988, Synthesis of late Paleozoic and Mesozoic eolian deposits of the Western Interior of the United States: Sedimentary Geology, v. 56, p. 3-125.

Breed C.S., Fryberger, G.S., Andrews, S., McCauley, C., Lenwartz, F., Gebel, D., and Horstman, K., 1979, Regional studies of sand seas using Landsat (ERTS) imagery, *in:* McKee, E.D., ed., A study of Global Sand Seas: Professional Paper U.S. Geologic Survey, v. 1052, p. 21-51.

Bristow, C. S., 2009, Ground Penetrating Radar Theory and Applications: Amsterdam, Netherlands, Elsevier Sciences, 508 p.

Bristow, C.S., Chroston, P.N., and Bailey, S.D., 2000, The structure and development of foredunes on a locally prograding coast: insights from ground-penetrating radar surveys, Norfolk, UK: Sedimentology, v. 47, p. 923-944.

Brookfield, M.E., 1977, the origin of bounding surfaces in ancient aeolian sandstones: Sedimentology, v. 24, p. 303-332.

Botha, G.A., Bristow, C.S., Porat, N., Duller, G., Armitage, S.J., Roberts, H.M., Clarke, B.M., Kota, M.W., Schoeman, P., 2003, Evidence for dune reactivation from GPR profiles on the Maputaland coastal plain, South Africa, *in:* Bristow, C.S., and Jol, H.M., eds., Ground Penetrating Radar in Sediments: London, Geological Society, Special Publications, v. 211, p. 29-46.

Chan, M.A., 1989, Erg Margin of the Permian White Rim Sandstone, SE, Utah: Sedimentology, v. 36, p. 235-251.

Chan, M.A., and Kocurek, G., 1988, Complexities in eolian and marine interactions: Processes and eustatic controls on erg development: Sedimentary Geology, v. 56, p. 283-300.

Chepil, W.S., 1956, Influence of moisture on erodibility of soil by wind: Soil Science Society of America, v. 20, p. 288-292.

Condon, S.M., 1997, Geology of the Pennsylvanian and Permian Cutler Group and Permian Kibab Limestone in the Paradox Basin, Southeastern Utah and Southwestern Colorado: U.S. Geological Survey Bulletin; 2000-P, p. 1-37.

Cooke, R.U., Warren, A., Goudie, A.S., 1993, Desert Geomorphology: London, UCL Press.

Dickinson, W.R., and Lawton, T.F., 2003, Sequential intercontinental suturing as the ultimate control for Pennsylvanian Ancestral Rocky Mountain deformation: Geology, v. 31, p. 609-612.

Dickinson, W.R., Soreghan, G.S., and Giles, K.A., 1994, Glacio-eustatic origin of Permo-Carboniferous stratigraphic cycles: Evidence from the southern Cordilleran foreland region: The Society for Sedimentary Geology, Tectonic and Eustatic Controls on Sedimentary Cycles, SEPM Concepts in Sedimentology and Paleontology #4, p. 25-34.

Ewing, R.C., Kocurek, G., and Lake, L.W., 2006, Pattern analysis of dune-field parameters. 713 Earth Surf. Proc. Land., 31, 1176-1191.

Fryberger, S.G., 2000, Geologic overview of White Sands National Monument: https://www.nature.nps.gov/geology/parks/whsa/geows/

Fryberger, S.G., Ahlbrandt, T.S., and Andrews, S., 1979, Origin, sedimentary features, and significance of low-angle eolian ‘sand sheet; deposits, Great Sand Dunes National Monument and vicinity, Colorado: Journal of Sedimentary Petrology, v. 49, p. 733-746.

Fryberger, S.G., Hesp, P., Hastings, K., 1992, Aeolian granule ripple deposits, Namibia: Sedimentology, v. 39, p. 319-331.

Fryberger S.G., Schenk, S.G., Krystinik, L.F., 1988, Stokes surfaces and the effects of near-surface groundwater-table on aeolian deposition: Sedimentology, v. 32, p. 21-41.

Harari, Z., 1996, Ground-penetrating radar (GPR) for imaging stratigraphic features and groundwater in sand dunes: Journal of Applied Geophysics, v. 36, p. 43-52.

Holm, D.A., 1960, Desert geomorphology in the Arabian Peninsula: Science, v. 132, p. 1369-1379.

Howell, J., and Mountney, N.P., 1997, Climactic cyclicity and accommodation space in arid to semi-arid depositional systems: an example from the Rotliegend Group of the UK southern North Sea, *in:* Zeigler, K., Turner, P., and Daines, S.R., eds., Petroleum Geology of the Southern North Sea: Future Potential: London, Geological Society, v. 123, p. 63-86.

Hunter, R.E., 1977, Basic types of stratification in small eolian dunes: Sedimentology, v. 24, p. 361-387.

Hunter, R.E., Richmond, B.M., Alpha, T.R., 1983, Storm-controlled oblique dunes of the Oregon coast: Geological Society of America Bulletin, v. 94, p. 1350-1465.

Jerolmack, D.J., Ewing, R.C., Falcinin, F., Martin, R.L., Masteller, C., Phillips, C., Reitz, M.D., Buynevich, I., 2012, Internal boundary layer model for the evolution of desert dune fields: Nature Geoscience, v. 5, p. 206-209.

Jol, H.M. and Bristow, C.S., 2003, GPR in sediments: Advice on data collection, basic processing and interpretation, a good practice guide, *in*: Bristow, C.S. and Jol, H.M., eds., Ground Penetrating Radar in Sediments, Geological Society, London, Special Publication 211, p. 9–27.

Jordan, O.D., and Mountney, N.P., 2010, Styles of interaction between aeolian, fluvial, and shallow marine environments in the Pennsylvanian to Permian lower Cutler beds, south-east Utah, USA: Sedimentology, v. 57, p. 1357-1358.

Jordan, O.D., and Mountney, N.P., 2012, Sequence stratigraphic evolution and cyclicity of an ancient coastal desert system: The Pennsylvanian-Permian lower Cutler

beds, Paradox basin, Utah, U.S.A.: Journal of Sedimentary Research, v. 82, p. 755-780.

Kluth, C.F., and Coney, P.J., 1981, Plate tectonics of the Ancestral Rocky Mountains: Geology, v. 9, p. 10-15.

Kocurek, G., 1999, The aeolian rock record (Yes, Virginia, it exists, but it really is rather special to create one): Aeolian environments, sediments and landforms, p. 239-259.

Kocurek, G. and Ewing, R.C., 2017, Trickle-Down and Trickle-Up Boundary Conditions in Eolian Dune-Field Pattern Formation: SEPM Special Publications, v. 108.

Kocurek, G. and Lancaster, N, 1999, Aeolian system sediment state: theory and Mojave Desert Kelso dune field example: Sedimentology, v. 46, p. 505-515.

Kocurek, G., and Neilson, J., 1986, Conditions favourable for the formation of warm-climate aeolian sand sheets: Sedimentology, v. 33, p. 795-816.

Kocurek G., Carr, M., Ewing, R., Havholm, K.G., Nagar, Y.C., Singvi, A.K., 2007, White Sands Dune Field, New Mexico: Age, dune dynamics and recent accumulations: Sedimentary Geology, v. 197, p. 313-331.

Kocurek, G. Townsley, M., Yeh, H., Havholm, K., and Sweet, M.L., 1992, Dune and dune-field development on Padre Island, Texas, with implications for interdune deposition and water-table-controlled accumulation: Journal of Sedimentary Petrology, v. 62, p. 622-635.

Kroy, K., Sauermann, G., Herrmann, H.J., 2002, Minimal model for sand dunes: Physical Review, v. 66 031302, p. 1-18.

Lancaster, N., 1982, Dunes on the Skeleton Coast, Namibia (South West Africa): Geomorphology and grain size relationships: Earth Surface Processes and Landforms, v. 7, p. 575-587.

Lancaster, N., 1996, Field studies of sand Patch initiation processes on the northern margin of the Namib Sand Sea: Earth Surface Processes and Landforms, v.21, p. 847-954.

Langford, R.P., 2003, The Holocene history of the White Sands dune field and influence on eolian deflation and playa lakes: Quaternary International, v. 104, p. 31-39.

Langford R.P., and Chan, M.A., 1993 Downwind Changes within an Ancient Dune Sea, Permian Cedar Mesa Sandstone, Southeast Utah *in:* Pye, K., and Lancaster, N., eds., Aeolian Sediments: Ancient and Modern: Oxford, U.K., Blackwell Publishing Ltd., ch. 8.

Lawton, T.F., Buller, C.D., and Parr, T.R., 2015, Provenance of a Permian erg on the western Margin of Pangea: Depositional System of the Kungurian (late Leonardian) Castle Valley and White Rim sandstones and subjacent Cutler Group, Paradox Basin, Utah, USA: Geosphere, v. 11, p.1475-1506.

Leclair, S.F., and Bridge, J.S., 2001, Quantitative interpretation of sedimentary structures formed by river dunes: Journal of Sedimentary Research, v. 71, p. 713-716.

Loope, D.B., 1984, Eolian origin of the Upper Paleozoic sandstones, southeastern Utah: Journal of Sedimentary Petrology, v. 54, p. 563-580.

Loope, D.B., 1985, Episodic deposition and preservation of eolian sands: A late Paleozoic example from southeastern Utah: Geology, v. 13, p. 73-76.

Loope, D.B., Sanderson, G.A., Verville, G.J., 1990, Abandonment of the name Elephant Canyon Formation in southeastern Utah: physical and temporal implications: Mountain Geologists, v. 27, p. 119-130.

Mainguet, M., 1984, A classification of dunes based on aeolian dynamics and the sand budget: *in:* El-Baz, F., ed., Deserts and Arid Lands: Dordrecht, Martinus Nijhoff, p. 31-58.

McKee, E.D., 1966, Structures of dunes at White Sands National Monument, New Mexico: Sedimentology, v. 7, p. 1-69.

McKee, E.D., and Douglass, J.R., 1971, Growth and movement of dunes at White Sands National Monument, New Mexico: U.S. Geological Survey Professional Paper, v. 750-D, p. D-108-D114.

McKnight, E.T., 1940, Geology of the Area between Green and Colorado Rivers, Grand and San Juan Counties, Utah: Geologic Survey Bulletin, v. 908, p. 147.

Momiji, H., Nishimori, H., Bishop, S.R., 2002, On the shape and migration speed of a proto-dune: Earth Surface Processes and Landforms, Short Communication, v. 27, p. 1335-1338.

Mountney, N.P., 2006, Periodic accumulation and destruction of aeolian erg sequences: the Cedar Mesa Sandstone, White Canyon, southern Utah: Sedimentology, 53, 789-823.

Mountney, N.P., and Jagger, A., 2004, Stratigraphic evolution of an aeolian erg margin system: the Permian Cedar mesa Sandstone, SE Utah, USA: Sedimentology, v. 51, p. 1-31.

Nielson, J., and Kocurek, G., 1986, Climbing zibars of the Algodones, southeastern California: Sedimentary Geology, v. 48, p. 1-15.

Norris, R.M., and Norris, K.S., 1961, Algodones Dunes of Southern California: Geological Society of America Bulletin, v. 72, p. 605-620.

Paola, C. and Borgman, L., 1991, Reconstructing random topography from preserved stratification: Sedimentology, v. 38, p. 553-565.

Parkhomenko, E.I., 1967, Electrical Properties of Rocks: New York, Plenum Press.

Parteli, E.J.R., Durán, O., Herrmann, H.J., 2007, Minimal size of a barchan dune: Reply to Comment, Physical Review, v. 76 063302, p. 1-10.

Pederson, A., Kocurek, G., Mohrig, D., Smith, V., 2015, Dune Deformation in a multi-directional wind regime: White Sands Dune field, New Mexico: Earth Surface Processes and Landforms, v. 40, p. 925-941,

Peterson, F., 1988, Pennsylvanian to Jurassic eolian transportation systems of the western United States: Sedimentary Geology, v. 56, p. 207-260.

Rankey, E.C., 1997, Relationships between relative changes in sea level and climate shifts: Pennsylvanian-Permian mixed carbonate siliciclastic strata, western United States: GSA Bulletin, v. 109, p. 1089-1100.

Sharp, R.P., 1963, Wind ripples: Journal of Geology, v. 71, p. 617-636.

Sharp, R.P., 1964, Wind driven sand in the Coachella Valley, California: Geologic Society of America Bulletin, v. 75, p. 758-804.

Soreghan, G.S., Keller, R.G., Gilbert, C.M., Chase, C.G., and Sweet, D.E., 2012, Load-induced subsidence of the Ancestral Rocky Mountains recorded by preservation of Permian landscapes: Geosphere, v. 8, p. 654-668.

Soreghan, G.S., Soreghan, M.J., Hamilton, M.A., 2008, Origin and significance of loess in late Paleozoic western Pangea: A record of tropical Cold?: Paleogeography, Paleoclimatology, Paleoecology, v. 268, p. 234-259.

Soreghan, M.J., Soreghan, G.S., and Hamilton, M.A., 2002, Paleowinds inferred from detrital-zircon geochronology of upper Paleozoic loessite, western equatorial Pangea: Geology, v 30, p. 695-698.

Svasek, J.N., and Terwindt, J.H., 1974, Measurement of sand transport by wind on a natural beach: Sedimentology, v. 21, p. 311-322.

Warren, A., 1971, Dunes in the Tenere Desert: The Geographical Journal, v. 137, p. 458-461.

Wilson, I.G., 1971, Desert Sandflow Basins and a Model for the Development of Ergs: The Geographical Journal, v. 137, p. 180-199.

Wilson, I.G., 1972. Aeolian bedforms-their development and origins: Sedimentology, v. 19, p. 137-210

Wilson, I.G., 1973, Ergs: Sedimentary Geology, v. 10, p. 77-106.

Ye, H., Royden, L., Burchfiel, C., and Schuepbach, M., 1996, Late Paleozoic Deformation of Interior North America: AAPG Bulletin, v. 80, p. 1397-1432.

Young, K.F., and Frederikse, H.P.R. (1973) Compilation of the Static Dielectric Constant 783 of Inorganic Solids. J. Phys. Chem. Ref. Data, 2 (2), 313-409.